CONTAINMENT INTERNAL STRUCTURE: STIFFNESS AND DAMPING FOR ANALYSIS

MUAP-11018

Non-Proprietary Version

August 2011

Revision History

Revision	Page	Description
0	All	Initial Issue

Mitsubishi Heavy Industries, Ltd.
16-5, Konan 2-chome, Minato-ku
Tokyo 108-8215 Japan

Table of Contents

APPENDICES

LIST OF ACRONYMS

The following list defines the acronyms used in this document.

3-D	Three-Dimensional
ACI	American Concrete Institute
ASCE	American Society of Civil Engineers
CIS	Containment Internal Structure
CQC	Complete Quadratic Combination
DCD	Design Control Document
FE	Finite Element
ISRS	In-Structure Response Spectra
LOCA	Loss of Coolant Accident
LEFE	Linear Elastic Finite Element
OBE	Operating Basis Earthquake
PCCV	Prestressed Concrete Containment Vessel
R/B	Reactor Building
RC	Reinforced Concrete
RCL	Reactor Coolant Loop
RCS	Reactor Coolant System
RWSP	Refueling Water Storage Pit
SC	Steel-Concrete
SRSS	Square Root Sum of The Squares
SSE	Safe Shutdown Earthquake
SSI	Soil-Structure Interaction
US NRC	United States Nuclear Regulatory Commission
ZPA	Zero-Period Acceleration

LIST OF FIGURES

LIST OF TABLES

ABSTRACT

This technical report presents the development of appropriate structural stiffness and damping values for the Containment Internal Structure (CIS) of the US-APWR standard plant. These stiffness and damping values will be used for modeling the dynamic behavior of the CIS while conducting: (i) soil-structure interaction (SSI) analysis of the reactor building (R/B) complex, and (ii) subsequent structural analysis for calculating design force demands.

The report develops two sets of stiffness and damping values that are intended to capture the potential range of stresses and associated cracking levels in each of the different concrete structure types (or categories) in the CIS, including various reinforced concrete (RC) structures and the steel-concrete (SC) primary and secondary shielding walls. The first set of values represents the limited concrete cracking and higher stiffness anticipated for seismic loading during normal plant operations, and the second set of values represents the significant reduction in stiffness associated with extensive concrete cracking under seismic loading coupled with accident thermal conditions. The category-specific stiffness and damping values identified for each of these two conditions are based upon stress levels calculated in the basic design analyses. Appropriate values for the extent of cracking indicated by these stress levels are then assigned to the RC structures (and other structures deemed to behave like RC) in accordance with available codes and regulatory guidance. The values assigned to the SC structures are based on experimentally verified stiffnesses that are similar in magnitude to those codified for RC structures, with small variations that are directly attributable to experimentally observed differences in SC behavior.

EXECUTIVE SUMMARY

The US-APWR CIS is a complex structure that includes six different structure categories: (1) steel-concrete (SC) composite walls with thickness less than or equal to 56 in., (2) SC-type walls with thickness greater than 56 in., (3) SC-type primary shield structure with three steel plates and thickness from 10-15 ft, (4) reinforced concrete slabs, (5) massive reinforced concrete structures, and (6) steel structures with non-structural concrete filling.

A significant portion of the CIS consists of 48 in. thick SC walls. Some small portions of the CIS utilize thicker (58 – 67 in.) SC walls. The primary shield structure supporting the reactor vessel is an SC-type structure consisting of three steel plates (one on each surface and one in the middle) and about 10 – 15 ft. overall thickness. All the floor slabs are made from conventional reinforced concrete. Towards the base of the CIS, the refueling cavity, the steam generators, and the reactor coolant pumps are supported on massive reinforced concrete infills. Additionally, the CIS involves some steel structures (e.g., floor grids) with plain concrete infill for radiation shielding.

This report presents the approach for estimating the structural stiffness and damping values of the various structure categories of the CIS, and modeling them using linear elastic finite element (LEFE) models to determine: (i) the in-structure response spectra for equipment design and qualification, and (ii) seismic and structural force demands for design.

The stiffness and damping values are commensurate with the level of concrete cracking expected to occur in the various structure categories of the CIS. The extent of concrete cracking depends on the (ACI 349) loading combinations for designing the CIS. Two basic loading combinations dominate: (A) seismic plus operating thermal, and (B) seismic plus accident thermal loading. These are referred to as condition “A” and condition “B”, respectively, in the report.

The report presents the stiffness and damping values for all the structure categories of the CIS while accounting for the extent of concrete cracking associated with loading conditions “A” and “B”.

It is important to note that the Category 1-3 SC-type walls are similar to reinforced concrete (RC) walls conventionally used in safety-related nuclear facilities. They both consist of thick concrete walls that are reinforced by steel. In SC walls, the concrete is reinforced with steel faceplates that are anchored to the concrete using shear studs and connected to each other using steel tie bars. In RC walls, the concrete is reinforced with orthogonal grids of deformed steel rebars that are embedded into the concrete will clear cover, and arranged to provide curtains of steel reinforcement close to each wall surface.

The behavior of SC-type walls is similar to that of equivalent RC walls. The extent of concrete cracking and its influence on the structural stiffness and damping will also be similar. However, some aspects of SC specific behavior can cause slight deviations from RC behavior. For example: (i) The SC steel plates provide additional in-plane shear stiffness due to their continuous nature. (ii) The bond between SC steel plates and concrete will be intermittent (discontinuous) at shear connector locations. (iii) The steel reinforcement ratios for SC walls are much higher (about 2-4%).

The behavior of SC walls subjected to in-plane and out-of-plane forces and thermal loading has been studied experimentally in Japan and the US. Based on these experimental evaluations, some SC specific equations have been developed to represent their in-plane shear and flexural stiffness before and after cracking. The development of these equations and their correlation with experimental data has been presented in this report for reference.

However, more importantly, the report includes comparisons of the stiffness values calculated using SC specific equations and those estimated using RC behavior. These comparisons are very important because they demonstrate that in spite of SC specific behavior, the deviations from RC behavior are quite small and easily justifiable. They also verify the adequacy of using RC wall stiffness equations published in ASCE 43-05 for SC walls specific to the US-APWR CIS. The US-APWR project chose to use the SC specific stiffness and damping values for the Category 1 walls because they capture SC wall behavior more appropriately and are experimentally verified for the range of material and geometric parameters in use.

The table below summarizes the SC specific stiffness equations for the Category 1 SC walls. It also includes the corresponding RC wall stiffness equations. It is evident from the equations that the RC wall equations do not account for the steel reinforcement ratio, or the special composite behavior of SC walls.

Structure Category	Loading Condition A ($E_{ss} + T_o$)			Loading Condition B ($E_{ss} + T_a$)		
	Shear Stiffness	Flexural Stiffness	Damping	Shear Stiffness	Flexural Stiffness	Damping
1 SC specific	Uncracked SC $G_cA_c + G_sA_s$	Cracked-SC E_cI_{ct}	4%	Cracked SC $0.5\,\overline{\rho}^{-0.42}\left(A_sG_s\right)$	Cracked-SC E_cI_{ct}	5%
1 RC wall	Uncracked G_cA_c	Uncracked E_cI_g	4%	Cracked $0.5G_cA_g$	Cracked $0.5E_cI_g$	7%

For the reinforcement ratios (1.8-4.2%) used in the US-APWR project, this limitation does not have a significant influence. This is demonstrated in the following table, which includes the calculated stiffness values for the typical US-APWR SC wall with 48 in. thickness, 0.5 in. thick steel plates (2% reinforcement ratio), and 4000 psi concrete strength.

As shown, for condition “A”, the SC specific in-plane shear stiffness and axial stiffness are within 13% of the corresponding RC values, and the SC specific flexural stiffness is 67% of the corresponding RC value. The slightly lower flexural stiffness is due to the fact that SC walls tend to crack early in flexure due to locked in shrinkage strains and lower degree of composite action. For condition “B”, the SC specific in-plane shear and axial stiffness are within 16% of the corresponding RC values, and the SC specific flexural stiffness is about 34% larger than the corresponding RC values. The slightly higher flexural stiffness is due to the higher reinforcement ratio (2%) in SC walls.

The most important comparisons in the table above are those related to the in-plane shear stiffness, because they dominate the lateral load (seismic) behavior of the CIS. As shown the in-plane shear stiffness calculated using SC specific equations were within 13-16% of the corresponding RC values. This further verifies the adequacy of using either the SC specific or the RC wall stiffness equations published in ASCE 43-05 for SC-type walls specific to the US-APWR project (reinforcement ratios 1.8-4.2%).

Based on this discussion, for Category 2 and 3 SC-type walls, the stiffness and damping values are based on those of RC walls published in ASCE 43-05, and summarized as follows:

Structure Category	Loading Condition A ($E_{ss} + T_o$)			Loading Condition B ($E_{ss} + T_a$)		
	Shear Stiffness	Flexural Stiffness	Damping	Shear Stiffness	Flexural Stiffness	Damping
2	Uncracked RC G_cA_c	Uncracked RC E_cI_c	4%	Cracked RC 0.5 G_cA_c	Cracked RC 0.5 E_cI_c	7%
3	Uncracked RC G_cA_c	Uncracked RC E_cI_c	4%	Uncracked RC G_cA_c	Uncracked RC E_cI_c	4%

The Category 2 SC-type walls are demonstrated in this report to remain effectively uncracked for loading condition “A”. They are assumed to be fully cracked for loading condition “B”. The Category 3 primary shield structure SC-type walls are demonstrated to remain uncracked for both loading conditions “A” and “B” in the report. For loading condition “B” (accident thermal), the primary shield structure remains uncracked due to significant restraint from the surrounding massive RC structure, and its large thickness.

The stiffness and damping values for category 4 and 5 RC structures are based on values published in ASCE 43-05, and summarized as follows.

Structure Category	Loading Condition A ($E_{ss} + T_o$)			Loading Condition B ($E_{ss} + T_a$)		
	Shear Stiffness	Flexural Stiffness	Damping	Shear Stiffness	Flexural Stiffness	Damping
4	Uncracked RC G_cA_c	Uncracked RC E_cI_c	4%	Uncracked RC G_cA_c	Cracked RC 0.5 E_cI_c	7%
5	Uncracked RC G_cA_c	Uncracked RC E_cI_c	4%	Uncracked RC G_cA_c	Uncracked RC E_cI_c	4%

The Category 4 RC slabs are demonstrated in this report to remain effectively uncracked for loading condition “A”. They are assumed to be cracked in flexure for loading condition “B”. The Category 5 massive RC structures are assumed to remain uncracked for both loading conditions “A” and “B” in the report due to their significant size, thermal inertia, and thickness.

The stiffness and damping values for Category 6 steel structures with non-structural concrete infill are based on the stiffness of the steel structure alone. The mass associated with the non-structural concrete infill is included directly in the models, but the concrete is not accorded any structural stiffness.

Thus, the stiffness and damping values for the different structure categories of the CIS are based on experimental results, understanding of structural behavior, good engineering judgment, and deliberate use of reinforced concrete standards and codes endorsed by the US-NRC. The development of these stiffness and damping values are presented in more technical detail in the report.

1.0 INTRODUCTION

1.1 Purpose

The purpose of this report is to define appropriate stiffness and damping values for use in structural analysis of the US-APWR Containment Internal Structure (CIS). Within the overall CIS design and validation methodology presented in Technical Report MUAP-11013 (Reference 1), this report presents the basis for the structural properties assigned to the finite element (FE) analysis models that support Task 1-A, “Dynamic Soil-Structure Interaction (SSI) Analysis”; and Task 1-B, “Seismic Analysis for Structural Design”, both of which are described in Reference 1.

1.2 Objectives

The fundamental goal of the Task 1 analyses is to accurately characterize the seismic demands on the structural members of the CIS and the critical equipment they support, including the reactor and the reactor coolant system (RCS). As both Tasks 1-A and 1-B will employ linear elastic finite element (LEFE) models to achieve this goal, it is necessary to calculate effective stiffness values that reflect the extent of concrete cracking anticipated in the CIS during the seismic response. Once the cracked stiffness values are ascertained, appropriate damping values are assigned that reflect the energy dissipation capability of the cracked members.

As explained in MUAP-11001 (Reference 2), the finite element models used for the SSI and subsequent structural analyses will be three-dimensional (3D) LEFE models. They will not be lumped mass stick models due to the limitations of such models. Assessing the effects of concrete cracking on stiffness of the 3D LEFE models is not straightforward because the CIS is made up of different structure categories that have varying response levels under applied loads and thermal conditions. For example, an overall percentage-type stiffness reduction would not be appropriate because of the varying responses of different structure categories under applied loads and thermal conditions. Similarly, the $1/10^{th}$ scale test of a related CIS structure presented in MUAP-11005 (Reference 3) cannot be used to estimate the stiffness for the 3D LEFE models because: (1) It measures and provides only the overall (lumped) stiffness of the structure, not the stiffness of the individual members (walls etc.) of different categories. (2) The test structure had some deviations from the US-APWR CIS, which further limit the use of the overall structure stiffness. And, (3) the $1/10^{th}$ scale test does not include the combined effects of three spatial earthquake components, or the effects of thermal conditions on the overall stiffness. Therefore, the approach for defining stiffness values for the CIS must meet the following objectives:

1. Best-estimate stiffness values must be calculated for each of the structure categories in the CIS (as described in Section 2.0 below), based on their unique behavioral characteristics.

2. The stiffness values estimated for each category must account for the range of concrete stresses and resulting concrete cracking levels anticipated for the seismic loading conditions to which the structure may be exposed, including:
    - Seismic loading during normal operations
    - Seismic loading during Loss of Coolant Accident (LOCA) conditions.

The variation in stiffness values produced by these two conditions necessitates two separate analyses, and the results of these analyses must be enveloped.

3. For structures in which the best-estimate stiffness values approach the uncracked or cracked values, a bounding analysis approach should be applied wherein the uncracked stiffness is used in the first analysis and the cracked stiffness is used in the second analysis. This ensures that inherent uncertainties in the loading inputs and analysis methods do not result in underestimated demands. The conservatism of this bounding approach must be verified by ensuring that the input motion dominant frequency does not fall within the range of fundamental frequencies produced by the uncracked and cracked stiffness estimates.

4. The stiffness and corresponding damping values estimated for each of the two analyses should be applied consistently to the models supporting Tasks 1-A and 1-B. Damping values assigned to the SSI analysis model (Task 1-A) must be appropriate for generation of in-structure response spectra (ISRS), in accordance with Regulatory Guide 1.61 (see Reference 4).

1.3 Approach and Report Overview

The following steps were taken to meet the objectives stated above for characterizing the CIS stiffness and damping, and will be described in detail in this report:

1. *Define Structure Categories*: Define the structure categories in the CIS in order to differentiate and group the walls and slabs based on their expected behavior. This step is discussed in Section 2.
2. *Define Loading Conditions*: In consideration of the design load combinations for the CIS, identify the basic loading conditions that must be considered to assess the potential range of concrete stresses and attendant cracking in each of the structure categories. This step is discussed in Section 3.
3. *Define Category-Specific Stiffness and Damping*: Define stiffness equations and damping values that are specific to each structure category. These are obtained from available codes and/or regulatory guidance for RC structures and are based upon experimentally verified values for SC structures. This step is discussed in Section 4.
4. *Evaluate Seismic + Normal Operating Condition*: Estimate the extent of cracking for seismic loading during normal operating conditions and assign appropriate stiffness and damping values for each category. This step is discussed in Section 5.
5. *Evaluate Seismic + Accident Condition:* Estimate the extent of cracking for seismic loading combined with accident conditions and assign appropriate stiffness and damping values for each structure category. This step is discussed in Section 6.
6. *Summarize Estimated Values:* Summarize the stiffness and damping values assessed for the two loading conditions and evaluate the feasibility of assigning overall damping ratios for each of the two corresponding analyses that would be appropriate for both ISRS generation and structural design. This step is discussed in Section 7.
7. *Application:* Apply the summarized stiffness and damping values to the analysis models. Calculate equivalent material properties for each wall and slab geometry that will produce the required stiffness terms and assign the properties to the elements of the Task 1A and 1B LEFE models. This step is discussed in Section 8.

2.0 STRUCTURE CATEGORIES[1]

As discussed above, the US-APWR CIS is comprised of a variety of structure types with significant differences in their construction and expected behavior. The structures in the CIS are classified into six categories to enable the use of appropriate analysis models and design methodologies for each of the structure categories. These six structure categories include three SC-type and three non-SC type categories, as explained in the following sub-sections. Figures 2-1 through 2-7 show several plan and elevation views of the US-APWR CIS that identify the six structure categories using a color-coded scheme. These figures have been developed from the drawings provided in References 5 and 6.

2.1 SC-type Structure Categories

The composite stiffness and strength of SC walls have been thoroughly established in experiments involving walls with overall thickness less than or equal to 56 in. Typical SC designs evaluated in these experiments consist of a single concrete core sandwiched between two steel faceplates, as shown in Figure 2-8. The steel faceplates are typically connected to the concrete core using headed stud anchors or embedded steel shapes, and the two steel faceplates are typically connected to each other using embedded steel shapes, tie bars, or web plates. The steel faceplate reinforcement ratios (ρ) in the experimental database vary between 1.5% and 5.0%, with ρ defined as follows:

Equation (2-1)

$$\rho = \frac{2 \cdot t_p}{T}$$

where t_p is the single faceplate thickness and T is the thickness of the overall section.

Most of the SC-type walls in the US-APWR CIS have material and geometric parameters that are within the range evaluated by the aforementioned experimental database. However, some of the walls have overall thicknesses and/or steel plate geometries that exceed this range. In these cases the fully composite stiffness cannot be assumed. Hence, the SC-type walls in the CIS are divided into the following three categories:

Category 1: *SC Walls with thickness less than or equal to 56 in.* These SC walls have material and geometric parameters that are within the range of the experimental database. This category includes the majority of the secondary shielding walls in the CIS. The most common SC wall is 48 in. thick, with 0.5 in. thick steel faceplates.

Category 2: *SC Walls with thickness greater than 56 in.* This category includes a relatively small portion of the CIS SC walls with thicknesses ranging from 58.5 in. to 67 in.

Category 3: *Primary Shield Walls.* The primary shield walls below elevation 35'-11" range in thickness from 9'-11" to 15'-4". They have a multi-cellular arrangement comprised of two steel faceplates, a mid-thickness steel plate, and numerous transverse web plates.

[1] The information in this section is also provided in Technical Report MUAP-11013 (Reference 1). It is repeated in this report for clarity.

2.2 Non-SC Structure Categories

The non-SC type walls in the CIS are classified into three additional structure categories:

Category 4: RC s*labs.* Standard RC floor slabs are used at various elevations throughout the CIS.

Category 5: *Massive reinforced concrete.* This category includes the thick reinforced concrete blocks at the base of the CIS that support the steam generators and reactor coolant pumps. These blocks are nominally 8 ft. to 32 ft. deep and are anchored to the basemat of the reactor building complex with steel reinforcement.

Category 6: *Steel structures with nonstructural concrete infill*. These structures consist of steel plates or steel shape grillages with nonstructural concrete provided for shielding purposes.

The US-APWR CIS also includes steel members that support the elevated reinforced concrete slabs at elevations 50'2" and 76'-5", as well as extensive secondary framing provided for support of operating platforms at various elevations. The columns that support the perimeter of the reinforced concrete slabs are explicitly modeled in the SSI and detailed design models in order to provide the correct vertical load path and boundary conditions for the slabs, but the rest of the secondary framing is included only as mass. In either case, the relative contribution of the steel framing stiffness and damping to the dynamic response of the primary structure is considered insignificant, such that these members are not included in the major structure categories identified for evaluation in this report.

Figure 2-1 CIS Structure Categories, Elevations 3'-7" to 21'-0"

Figure 2-2 CIS Structure Categories, Elevations 21'-0" to 35'-11"

Figure 2-3 CIS Structure Categories, Elevations 37'-9" to 62'-4"

Figure 2-4 CIS Structure Categories, Elevations 62'-4" to 76'-5"

Figure 2-5 CIS Structure Categories, Elevations 76'-5" to 139'-6"

Figure 2-6 CIS Structure Categories, Centerline Section Looking West

Figure 2-7 CIS Structure Categories, Centerline Section Looking North

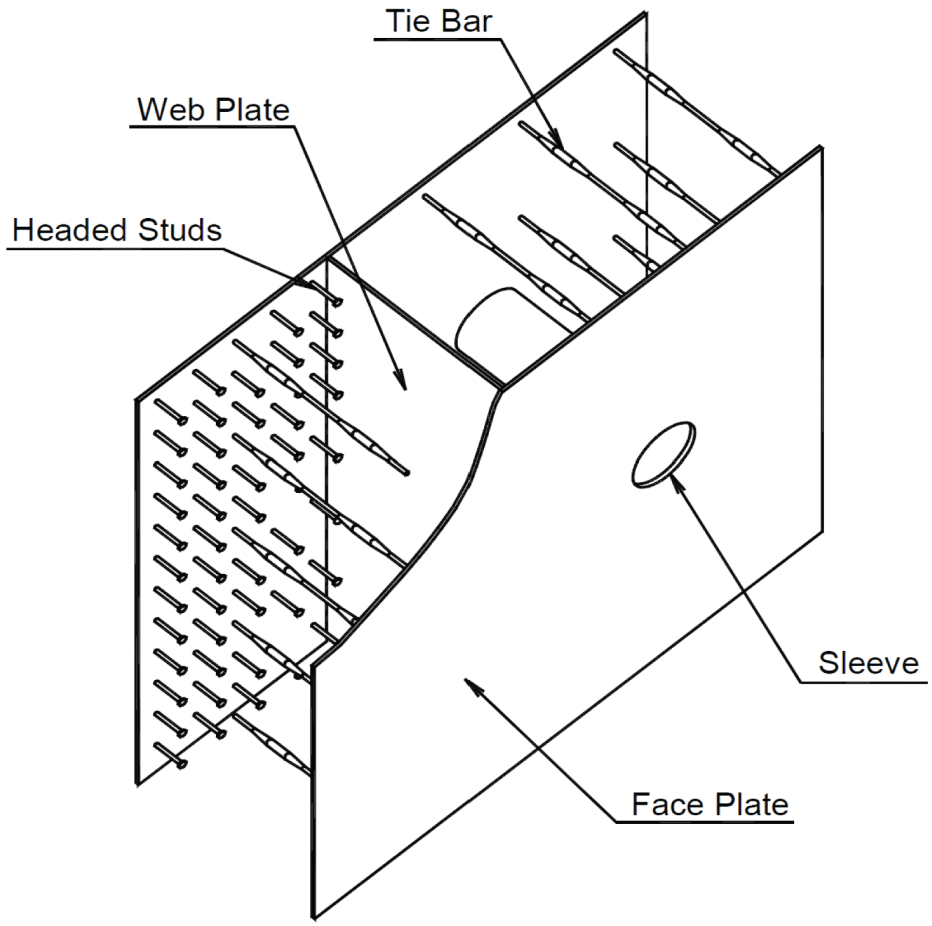

Figure 2-8 Typical SC Module Geometry

3.0 LOADING CONDITIONS FOR ASSESSMENT OF CRACKING

Assessment of load-induced concrete cracking for the CIS originates with identifying the specific load cases that will cause stresses that exceed the cracking stress of concrete and the combinations of these load cases that must be considered per regulatory guidance.

3.1 Design Load Combinations

The factored design load combinations for the CIS are governed by US Nuclear Regulatory Commission (US NRC) Regulatory Guide 1.142 (Reference 7) which states that concrete structures within a containment structure may be designed in accordance with the strength design provisions of American Concrete Institute (ACI) 349-97 (Reference 8). Regulatory Guide 1.142 approves the load combinations given in Section 9.2.1 of ACI 349-97, which are the same as those provided in the ACI 349-01 (Reference 9) code specified for use on the US-APWR project.[2] Several load factor modifications are required per the regulatory guide, which are included in the table of load combinations given in Table 3-1.

The site-independent seismic design of the US-APWR sets the operating-basis earthquake (OBE) ground motion at one-third of the safe-shutdown earthquake (SSE). This eliminates the requirement for performing explicit design analysis and load combinations containing OBE. As a result, the design load combinations that contain seismic loading are condensed to combinations 4 and 8 in Table 3-1. The evaluation of stiffness and damping for the CIS must address the extent of concrete cracking resulting from these two load combinations.

Besides seismic loading (E_{ss}), the most significant load cases in these two load combinations in terms of their potential to crack the thick concrete members of the CIS are the thermal loads, including operating thermal loads (T_o) and accident thermal loads (T_a). The results from analysis of the CIS prepared for basic design (see Reference 11) indicate that static dead (D), live (L), fluid (F), and accident pressure (P_a) loads result in minimal stress levels that will not cause significant concrete cracking in any of the CIS structures. As a result, loading combinations 4 and 8 from Table 3-1 may be reduced to the following basic loading conditions for assessment of concrete cracking in the CIS:

Condition “A”: $E_{ss} + T_o$

Condition “B”: $E_{ss} + T_a$

The following sections provide the details specific to the US-APWR CIS for each of the load cases in these two basic loading conditions.

3.2 CIS Seismic Loading

The CIS is a Seismic Category I structure to be evaluated for SSE seismic loading in accordance with Regulatory Guide 1.29 (Reference 12). Due to the irregularity of mass and stiffness in the CIS structure and the supported Reactor Coolant Loop (RCL), a dynamic analysis is used to determine the load path characteristics of the CIS. This analysis is performed using three-dimensional (3-D) finite element models developed for SSI analysis (Task 1A) and structural design (Task 1B).

[2] It is noted that future revisions of the US-APWR Design Control Document (DCD) will reference the load combinations in Appendix C of the ACI 349-06 code (Reference 10). These combinations are identical to those given in Reference 8 and Reference 9 for the loads applied to the US-APWR CIS.

A series of site-independent SSI analyses are performed for the reactor building complex using eight generic soil profiles. These analyses are performed with the ACS SASSI program using a coarse-meshed 3-D finite element model that includes the reactor building mat, the reactor building, the Prestressed Concrete Containment Vessel (PCCV) and the CIS (see Reference 13). The dynamic properties of the CIS portion of the ACS SASSI model were derived from and validated against the detailed, refined mesh model developed in ANSYS for the CIS basic design (Reference 11).

The inertial seismic loading is obtained from the site-independent SSI analyses in the form of ISRS at the base of the CIS that are used as input to response spectrum analyses in ANSYS for structural design. ISRS are also obtained from the site-independent SSI analyses for design of equipment components and supports at various locations in the structure. The design ISRS represent the broadened and enveloped spectra generated for eight generic soil profiles, as discussed in Reference 13. The ACS SASSI analyses also provide enveloped time-history acceleration data at points throughout the CIS structure that are used to verify that the ANSYS response spectrum analyses sufficiently capture the accelerations resulting from the overall dynamic response of the soil-structure system.

Both the SSI and detailed ANSYS analyses consider the hydrodynamic response of the refueling water to seismic base motion. For purposes of assessing stiffness, the hydrodynamic response is computed for the operating condition, during which the refueling water is housed in the Refueling Water Storage Pit (RWSP). The hydrodynamic response of the refueling water consists of the response of the impulsive mass acting rigidly with the walls of the RWSP, and the very low frequency convective or “sloshing” response of the convective mass. The manner in which these masses were computed and included in the analysis models is further discussed in Reference 11.

3.3 CIS Thermal Loading

The two basic loading conditions identified for evaluation of CIS stiffness and damping are differentiated by the associated thermal conditions. The design temperatures for the various compartments of the CIS during normal operating and accident thermal conditions are calculated in Reference 14 and summarized in the sections below.

3.3.1 Normal Operating Thermal Loads

The normal operating design temperatures in all of the CIS compartments except the reactor cavity are 105°F in the winter and 120°F in the summer. Since the ambient temperatures in these secondary compartments are equal in magnitude at any point in time, the walls and slabs that form the compartments experience steady state, uniform through-thickness temperatures. As a result, no significant concrete cracking is anticipated that would reduce the in-plane stiffness of the secondary compartment walls and slabs. However, thermal growth due to the net increase from construction temperatures (70^oF) to operating temperatures may cause flexural cracking wherever the growth is restrained. A preliminary analysis of the CIS was performed to evaluate the extent of flexural cracking resulting from the 50^oF temperature increase caused by the summer operating condition. The minimal stresses shown in the analysis results indicate that this condition will not cause significant flexural cracking in any of the walls and slabs of the secondary CIS compartments.

The normal operating temperature in the reactor cavity is 150°F. This results in a linear temperature gradient through the thickness of the primary shield walls of 30^oF during summer operations and 45°F during winter operations. These shallow linear gradients through the thick

primary shield walls will not cause significant concrete cracking. Appendix 3 provides a detailed explanation for this assessment in which it is demonstrated that linear thermal gradients result in minimal changes to mechanical stresses caused by structural loads.

Given the limited effects of the uniform temperatures applied to most of the CIS and the shallow linear gradients applied to the primary shield structure, the normal operating thermal load case is assessed to cause minimal concrete cracking in the CIS. As a result, the extent of concrete cracking for Condition ”A” will be taken as that induced by safe-shutdown seismic loading only. This is consistent with the objective to treat Condition ”A” as a rational upper-bound stiffness condition, to be considered in conjunction with the reduced stiffness associated with Condition ”B”.

3.3.2 Accident Thermal Condition

The design accident thermal loading condition for the CIS occurs as a result of the postulated pipe ruptures associated with a LOCA. Time histories of the temperatures occurring in the compartments of the CIS following a high-energy pipe rupture in either the reactor cavity or steam generator compartments are calculated in Reference 14, and typical examples are presented in Figure 3-1. As shown, the ambient temperature inside the compartment containing the ruptured pipe increases to 580°F immediately after the pipe rupture occurs. Because the CIS compartments are open to a common atmosphere, the ambient temperature in adjacent compartments immediately increases from the operating temperature to 200°F, and then to 300°F within ten seconds.

As discussed in Section 6, these temperature time histories are input into heat transfer analyses to calculate the temperature gradients that form through the thickness of the walls and slabs of the CIS, and to determine the variation of these gradients with respect to time. In general, the steep parabolic gradients that develop shortly after the accident occurs induce high membrane tensile stresses that exceed the concrete cracking stress. In addition, the accident thermal condition causes a significant net temperature increase in the CIS walls and slabs, which results in significant thermal growth and flexural cracking where the growth is restrained. Further discussion of the specific effects of the accident thermal loading on each structure category is provided in Section 6.

Temperatures in compartment where pipe rupture occurs

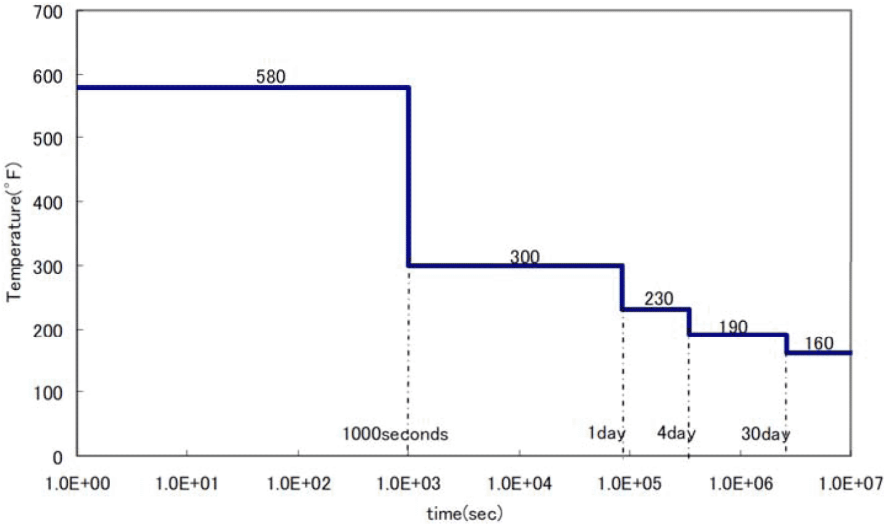

Temperatures in other compartments

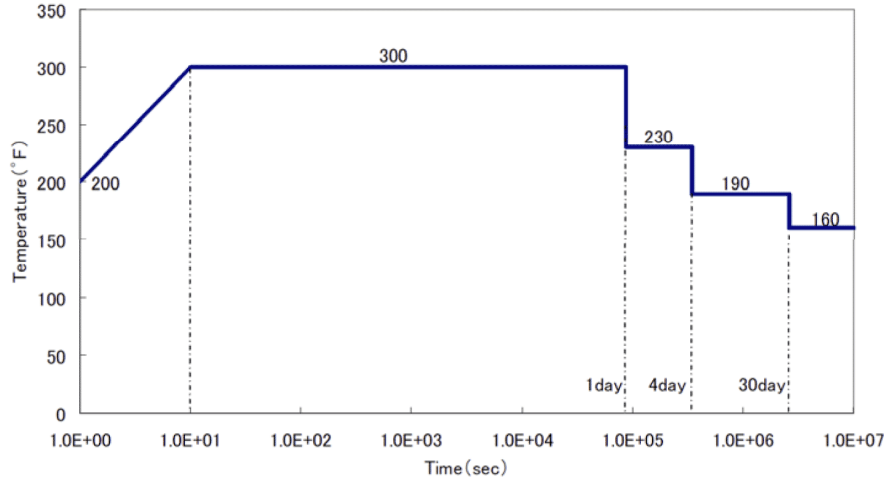

Figure 3-1 Temperature Time Histories for Accident Condition

1. $U = 1.4D + 1.4F + 1.7L + 1.7H + 1.7R_o$
2. $U = 1.4D + 1.4F + 1.7L + 1.7H + 1.7E_o + 1.7R_o$
3. $U = 1.4D + 1.4F + 1.7L + 1.7H + 1.7W + 1.7R_o$
4. $U = D + F + L + H + T_o + R_o + E_{ss}$
5. $U = D + F + L + H + T_o + R_o + W_t$
6. $U = D + F + L + H + T_a + R_a + 1.4P_a$
7. $U = D + F + L + H + T_a + R_a + 1.15P_a + 1.0(Y_r + Y_j + Y_m) + 1.15E_o$
8. $U = D + F + L + H + T_a + R_a + 1.0P_a + 1.0(Y_r + Y_j + Y_m) + 1.0E_{ss}$
9. $U = 1.05D + 1.05F + 1.3L + 1.3H + 1.2T_o + 1.3R_o$
10. $U = 1.05D + 1.05F + 1.3L + 1.3H + 1.3E_o + 1.2T_o + 1.3R_o$
11. $U = 1.05D + 1.05F + 1.3L + 1.3H + 1.3W + 1.2T_o + 1.3R_o$

Table 3-1 Design Load Combinations for the US-APWR CIS
As given in ACI 349-01 (Reference 9), with load factor modifications per RG 1.142 (Reference 7).)

4.0 CATEGORY-SPECIFIC STIFFNESS AND DAMPING

Before a detailed assessment can be made of the concrete cracking and associated stiffness reductions that result from the two loading conditions defined above, it is necessary to define generalized formulations for the stiffness and damping of each of the CIS structure categories. For the Category 1 SC walls, the stiffness and damping values are based on test results and verified models. As explained earlier, these stiffness and damping values are subsequently compared with those for equivalent RC structures to demonstrate their proximity and reasonableness. For the Category 2 and 3 SC walls, the stiffness and damping values of equivalent RC structures are used. For the Category 4 and 5 RC structures, the values used are those given in available codes and regulatory guidance for RC structures. The Category 6 structures are not modeled with any stiffness or damping for the nonstructural concrete; only the stiffness of the steel members is included. The following subsections provide further discussion of the basis for the individual stiffness and damping values considered for each structure category.

4.1 Category 1 SC Wall In-Plane Shear Stiffness

The in-plane shear stiffness of the Category 1 SC walls comprises the primary lateral load resisting mechanism for the US-APWR CIS and is therefore an essential component in the overall dynamic response of the structure. Modal analysis performed for the basic design (Reference 11) showed that the fundamental natural frequencies for lateral response of the CIS are directly related to the in-plane shear stiffness of these walls.

A reasonable characterization of SC wall in-plane shear stiffness must account for the significant contribution of the steel faceplates, both before and after cracking of the concrete core. The in-plane shear behavior of SC walls differs from that of RC walls because the continuous steel faceplates have a direct contribution to the in-plane shear stiffness of the composite wall. In RC walls, the reinforcing bars provide stiffness only in their axial directions and thus do not have a direct contribution to in-plane shear stiffness. It is important to note that the steel faceplates of SC walls are connected to the concrete infill and to each other with shear studs and tie bars. These connectors are typically designed to provide adequate composite action and strain compatibility between the steel plates and concrete infill as an engineering approximation. The experimental data discussed in the following sections demonstrate that composite action and strain compatibility (from an engineering perspective) can be achieved with reasonable shear stud size and spacing.

4.1.1 Uncracked In-Plane Shear Stiffness

Prior to cracking of the concrete core, the in-plane shear stiffness is estimated as the summation of the elastic shear stiffnesses of the concrete and steel, as follows:

(**Equation 4-1)** $$K_{uncr} = G_c A_c + G_s A_s$$

where G_c and A_c are the elastic shear modulus and cross-sectional area of the concrete core, respectively, and G_s and A_s are the corresponding values for the steel faceplates, per unit length of the wall.

In-plane shear tests performed by Ozaki et al. (see Reference 15) demonstrate that Equation 4-1 provides an accurate estimate of uncracked stiffness for typical SC wall geometries. As described in Appendix B, these tests used SC specimens with scaled

geometries similar to those of the US-APWR CIS Category 1 walls, including reinforcement ratios (ρ) between 2.3% and 4.5%, and anchorage stud pitch to faceplate thickness ratios (B/t) of 30 to 31. (Reinforcement ratios for the CIS Category 1 walls vary from 1.8% to 4.2%, and a maximum B/t ratio of 24 is to be provided). Figure B.4A in Appendix B shows that the experimental in-plane shear stiffness values observed prior to cracking compared favorably to values calculated using Equation 4-1.

4.1.2 In-Plane Shear Cracking Threshold

As shown in Appendix A, uncracked in-plane shear stiffness is considered for the Category 1 SC walls when applied in-plane shear forces are less than or equal to the cracking shear force:

(Equation 4-2) $$V_{ck} = 2\sqrt{f'_c}\left(A_c + \frac{G_s}{G_c}A_s\right)$$

where f'_c is the specified compressive strength of concrete in pounds per square inch (psi). The threshold for in-plane shear cracking is thus defined as the shear force causing a stress of $2\sqrt{f'_c}$ on the transformed area of the SC section.

For reinforced concrete applications, concrete cracking is typically assumed to occur when the maximum principal stress (which is equal to the shear stress for pure shear) exceeds the concrete tensile strength, equal to $4\sqrt{f'_c}$ (see Reference 16). As explained in Appendices A and B, the reduction of the cracking stress for SC sections to $2\sqrt{f'_c}$ is considered the result of locked-in tensile stresses in the concrete due to restraint of curing shrinkage by the steel faceplates. Thus the cracking shear force for SC sections may also be defined as follows:

(Equation 4-3) $$V_{ck} = (4\sqrt{f'_c} - \varepsilon_{sh}E_c)(A_c + \frac{G_s}{G_c}A_s)$$

where ε_{sh} is the shrinkage strain in the concrete section and E_c is the modulus of elasticity of concrete in psi. Since the tensile strength of concrete is itself highly variable and the magnitude of shrinkage strains is difficult to quantify, the experimental data for SC sections are seen as the most reliable indicator of the cracking threshold for in-plane shear. As shown in Figure 4-1, Ozaki et al. originally calculated the cracking shear force ('Q_c' in the nomenclature of Reference 15) in terms of a concrete stress of $4\sqrt{f'_c}$ (or approximately $0.33\sqrt{f'_c}$ for units of MPa). However, the experimental results clearly indicate cracking occurred nearer to a stress of $2\sqrt{f'_c}$ ($0.16\sqrt{f'_c}$ for units of MPa) as given in Equation 4-2.

4.1.3 Cracked In-Plane Shear Stiffness

After cracking of the concrete core due to applied in-plane shear forces, the concrete offers very little in-plane shear stiffness in the principal direction perpendicular to the plane of cracking. However, the concrete does contribute resistance to the applied shears in the direction parallel to the plane of cracking, as explained in Appendix A. This is referred to as cracked orthotropic behavior of the SC wall concrete core. For the case of pure shear, the orthotropic stiffness of the concrete manifests as compression struts that form between the diagonally oriented shear cracks. The formation of concrete compression struts is possible in

SC construction because the steel faceplates provide confinement to the struts as well as resistance of the tension tie forces in the idealized response of the wall as a truss.

The post-cracking composite in-plane shear stiffness of SC walls is derived in Appendix A. The resulting bilinear shear-deformation relationship is shown in Figure 4-3. The cracked tangent in-plane shear stiffness is equal to the sum of two terms representing the contributions of the steel faceplates (K_s) and the cracked concrete acting compositely with the steel plates (K_{sc}):

(Equation 4-4) $$K_{cr\_tan} = K_s + K_{sc}$$

where:

(Equation 4-5) $$K_s = A_s G_s$$

(Equation 4-6) $$K_{sc} = \frac{1}{\frac{4}{E'_c A_c} + \frac{2(1-\nu_s)}{E_s A_s}}$$

As presented in Appendix A, the post-cracking region of the bilinear shear-deformation curve terminates at the shear force that yields the steel faceplates according to the Von Mises yield criterion:

(Equation 4-7) $$V_n = \frac{K_s + K_{sc}}{\sqrt{3K_s^{\,2} + K_{sc}^{\,2}}} A_s F_y = \beta \cdot A_s F_y$$

wherein the following calibration parameters are defined:

(Equation 4-8) $$\beta = 1.11 - 5.16 \cdot \bar{\rho}$$

(Equation 4-9) $$\bar{\rho} = \frac{A_s F_y}{\sqrt{f'_c} A_c}$$

and F_y is the specified yield strength of the steel faceplates. For the faceplate reinforcement ratios used in the CIS Category 1 SC walls, the in-plane shear strength (V_n) is approximately equal to the yield strength of the steel plates (i.e. β is approximately equal to 1 and Equation 4-7 reduces to $V_n \approx A_s F_y$).

The theoretical composite response of SC walls to in-plane shear forces beyond the cracking threshold has been experimentally verified, both qualitatively and quantitatively. In the in-plane shear tests performed in Korea by Lee et al. (see Reference 17), removal of the steel faceplates from the specimens after testing revealed a grid of through-thickness cracks oriented at 45 degrees to the applied in-plane shear force, demonstrating the expected composite response and the formation of compressive struts (see Figure 4-2). Furthermore, the ultimate shear strengths exhibited by the specimens were approximately equal to the yield strength of the steel plates. This result is in accordance with Equation 4-7, given that these test specimens used similar reinforcement ratios to those specified for the US-APWR CIS. In

addition, the values observed in the Ozaki tests for post-cracking shear stiffness and the yielding shear force were closely approximated by Equations 4-4 and 4-7, respectively, as shown in Appendix B, Figures B.4b and B.4d.

For the linear elastic analyses to be performed in support of Tasks 1-A and 1-B, secant stiffness values must be assigned to the SC walls in order to obtain a reasonable assessment of the dynamic response for the anticipated level of cracking. Secant stiffness values are calculated on the basis of the applied in-plane shear forces in the manner illustrated by Figure 4-3; i.e. the applied shear force is plotted on the bilinear shear-deformation curve and the secant stiffness is calculated for that point.

As shown in Figure 4-4, the calculated secant stiffness values decrease rapidly for applied shear forces just beyond the cracking threshold, and then approach a relatively constant value for a large range of in-plane shear forces that are well beyond the cracking threshold. Hence it is possible to define an empirical, best-fit formula that provides a reasonable approximation of the so-called "fully cracked" secant stiffness for the range of parameters included in the experimental investigations (that is, reinforcement ratios between 2% and 4.5% and shear stud b/t ratios less than or equal to 30) :

(Equation 4-10)
$$K_{cr} = 0.5\left(\bar{\rho}^{-0.42}\right)G_s A_s$$

wherein a normalized reinforcement ratio is defined as:

(Equation 4-11)
$$\bar{\rho} = \frac{A_s F_y}{\sqrt{f'_c}\,A_c}$$

Further discussion of the basis for Equation 4-10 is provided in Appendix C. Figure 4-5 illustrates the calibration of Equation 4-10 to the fully cracked range of secant stiffness values for the typical 48"-thick Category 1 SC wall with ½"-thick faceplates. Section 6 of this report discusses the applicability of this equation to the Condition "B" analyses.

4.1.4 Effective In-Plane Shear Stiffness

As discussed in Section 5, the secant in-plane shear stiffness will be estimated for each of the Category 1 SC walls for Condition "A" on the basis of the seismic in-plane shear forces calculated from preliminary response spectrum analysis of the CIS. These in-plane forces represent the maximum forces that are postulated to occur at any time throughout the duration of seismic shaking. Therefore the secant stiffness calculated using these forces represents the minimum stiffness exhibited, and is only appropriate for the last portion of the largest response cycle. The stiffness exhibited by the walls for all other response cycles will be higher than the calculated value, as shown in Figures 4-5 and 4-6.

According to research prepared for reinforced concrete shear wall structures (see References 18 and 19), an effective stiffness value should be calculated for use in equivalent linear analyses that represents the aggregate of the stiffness values exhibited for all response cycles. The referenced research defined a calibrated relationship between effective linear stiffness and minimum secant stiffness by matching the maximum drift results obtained from a series of equivalent linear time-history analyses to those obtained with nonlinear time-history analyses. As discussed in Reference 19, for minimum secant stiffness values in the range of 0.25 to 1.0 times the initial stiffness, the calibrated relationship defined in the research can be approximated as follows:

(Equation 4-12)

$$\frac{K_{eff}}{K_{init}} = 1.25\frac{K_{sec}}{K_{init}} \le 1.0$$

where K_{eff} is the effective stiffness, K_{sec} is the minimum secant stiffness, and K_{init} is the initial stiffness. It is noted that this equation stipulates that the calculated effective in-plane shear stiffness must not exceed the initial stiffness, which is equal to the uncracked stiffness for Condition "A". Importantly, the initial stiffness for the thermal accident condition (Condition "B") is that induced by thermal cracking; it is not the uncracked stiffness. Therefore the stiffness values for Condition "B" will not be increased beyond the values associated with the thermally cracked condition.

Although the recommendations in the referenced research were specific to reinforced concrete shear walls, they are also considered appropriate for use with SC shear walls. Reference 19 acknowledges that the hysteresis loops for in-plane shear response of SC walls may be slightly less pinched than for reinforced concrete walls. However, this difference in behavior is deemed to have very little effect on the effective stiffness calibration presented in the research. It is only considered pertinent to the calculation of hysteretic damping.

4.1.5 Out-of-Plane Flexural Stiffness

As explained in Appendix E, experiments on SC walls subjected to out-of-plane flexure indicate that the uncracked composite flexural stiffness is never exhibited. Instead, the cracked composite stiffness is observed immediately upon application of loads that induce flexural stresses. There are several reasons given for this behavior. First, the concrete core of SC sections develops significant locked-in shrinkage stresses during casting. These stresses reduce the applied stress required to crack the concrete core. Also, the bond of the steel to the concrete in SC sections is not continuous as it is with deformed reinforcement in RC sections. Instead, the steel-concrete bond is intermittent, with connections only at the individual anchorage stud and tie bar locations. Since the anchorage studs have a certain degree of flexibility, a certain level of section rotation or slip is required to mobilize the steel

plate reinforcement. In the presence of locked-in shrinkage stresses, this rotation is sufficient to crack the concrete core prior to engagement of the reinforcement. Thus the uncracked composite stiffness of the SC section is never manifested.

As shown in Appendix E, the cracked composite flexural stiffness of SC walls may be approximated as the cracked-transformed flexural stiffness of the section. An empirical formula for the cracked-transformed stiffness is defined in Appendix E that distinguishes the steel and concrete stiffness contributions, as follows:

(Equation 4-13) $$EI_{cr\_tr} = E_s I_s + \alpha E_c I_c$$

where:

(Equation 4-14) $$\alpha = 0.48\rho' + 0.10$$

(Equation 4-15) $$\rho' = \frac{2t_p}{T}\frac{E_s}{E_c}$$

The calibration of the parameter 'α' to achieve the actual cracked-transformed stiffness values is illustrated in Appendix E. It is noted that α varies from 0.16 to 0.26 for the reinforcement ratios used by the Category 1 walls in the US-APWR CIS.

4.1.6 Axial Stiffness

Although the axial stiffness of the Category 1 SC walls is not considered to be as critical to the dynamic response of the CIS as the in-plane shear stiffness or out-of-plane flexural stiffness, the effects of concrete cracking on axial stiffness must still be considered. For the equivalent linear elastic analyses to be used for dynamic analysis of the CIS, the cracked axial stiffness assigned to the analysis models must try to capture both the reduced stiffness of the walls in tension and the gross stiffness of the walls in compression. Since this behavior can not be modeled explicitly, it may be argued that an equivalent axial stiffness should be assigned that is equal to the average of the cracked and uncracked stiffness values:

(Equation 4-16) $$EA_{avg} = \frac{1}{2}\left[E_s A_s + \left(E_s A_s + E_c A_c\right)\right] = E_s A_s + \frac{E_c A_c}{2}$$

However, this approach is somewhat questionable, since the portion of the walls closer to the base of the structure will have dead load compressions that may not be overcome by seismic uplift forces, and since the axial force resultants in the walls due to overturning will not be of uniform magnitude across the plan of the structure.

Given these uncertainties, the approach taken for modeling the axial stiffness of the Category 1 SC walls utilizes the elastic modulus (E) and cross sectional area (A) generated by matching the effective in-plane stiffness (GA) and out-of-plane flexural stiffness (EI) defined for each analysis condition. As will be further discussed in Section 8, this approach results in rational values of axial stiffness for both the uncracked analysis (Condition "A") and the cracked analysis (Condition "B").

4.1.7 Damping

As summarized in MUAP-10002 (see Reference 20), the energy dissipation capability of SC walls was evaluated in the 1/10th scale test of a containment internal structure performed by Akiyama et al. (see also Reference 21). An equivalent viscous damping factor for cracked SC walls was calculated from the observed hysteretic curves by equating the energy dissipated in the actual structure (i.e. the area enclosed by the hysteretic loop) to the energy dissipated in an equivalent viscous system. The associated equation given in Reference 21 is as follows:

(Equation 4-17)
$$h_{eq} = \frac{1}{2\pi} \cdot \frac{\Delta W}{W}$$

where ΔW is the area enclosed by the hysteretic loop and W is the strain energy for a complete cycle of the equivalent viscous system (see Figure 4-6). The equivalent viscous damping ratio calculated in Reference 21 using this equation was approximately 5%. This value is considered reasonable, given that it falls between the SSE damping values provided in Regulatory Guide 1.61 (Reference 4) for reinforced concrete and welded steel (7% and 4%, respectively).

The energy dissipation characteristics of uncracked SC walls are considered to be similar to those of uncracked reinforced concrete walls, for which a 4% damping ratio is given in Reference 4.

4.2 Stiffness and Damping of Category 2 and 3 Walls

As discussed above in Section 2.1, the experimental database that fully confirms the composite stiffness characteristics of SC walls before and after cracking is limited to sections with overall thickness less than 56 in. Some experimentation has been performed on the behavior of the primary shield structure (see Reference 22), but further study is required to ascertain that the composite behavior observed for this structure is fully consistent with that derived and experimentally verified for the Category 1 SC walls. Therefore the additional flexural and in-plane shear stiffness contributions from the steel plates will not be considered for the Category 2 and 3 walls. Instead, the stiffness and damping values for reinforced concrete will be used. The sources referenced for these values are discussed below.

4.3 Stiffness and Damping of Category 4 and 5 Reinforced Concrete Structures

Stiffness and damping values for reinforced concrete structures are provided in the currently available nuclear standards. Specifically, Table 3-1 of American Society of Civil Engineers (ASCE) 43-05 (Reference 23) provides out-of-plane flexure, in-plane shear, and axial stiffness values for RC walls and slabs. These values are restated in Table 4-1 of this report. It is noted that the code specifies the values to be used on the basis of anticipated cracking. For out-of-plane flexural stiffness, cracked values are specified if the bending stress in the slabs or walls exceed the cracking stress. Cracked in-plane shear stiffness values are specified when in-plane shear forces exceed the nominal concrete shear capacity.

Regulatory Guide 1.61 (Reference 4) provides damping values for reinforced concrete structures that are intended for use in Operating Basis Earthquake (OBE) analyses and Safe Shutdown Earthquake (SSE) analyses. The damping levels specified (4% for OBE and 7% for SSE) are based on the expectation of limited cracking during response to the OBE

accelerations, and extensive cracking associated with responses close to code stress limits under SSE loading.

In keeping with the approach identified in these standards, stiffness and damping values will be assigned to the structures of the CIS for each of the two loading conditions considered on the basis of anticipated cracking. The assessment of cracking for each condition is described in Sections 5 and 6.

4.4 Category 6 Modeling

As stated above, the Category 6 structures in the CIS consist of grillages of steel plates or shapes (e.g. wide-flange sections) that are filled with concrete for shielding purposes. The concrete in these structures is nonstructural, as it is not detailed to act compositely with the steel. Hence the CIS analysis models for Tasks 1A and 1B will include the stiffness of the steel members only. The concrete infill will be considered only as lumped mass on the steel structures.

Figure 4-1 Calculated vs. Experimental Cracking Shear Force
As presented in Reference 15; Q_c is defined as the “cracking strength” and is equal to the term V_{ck} defined in Equation 4-2 in this report.)

Figure 4-2 Diagonal Cracking Pattern in SC Panel Subjected to In-Plane Shear
As shown in Reference 17. The steel faceplate has been removed to observe the concrete core.

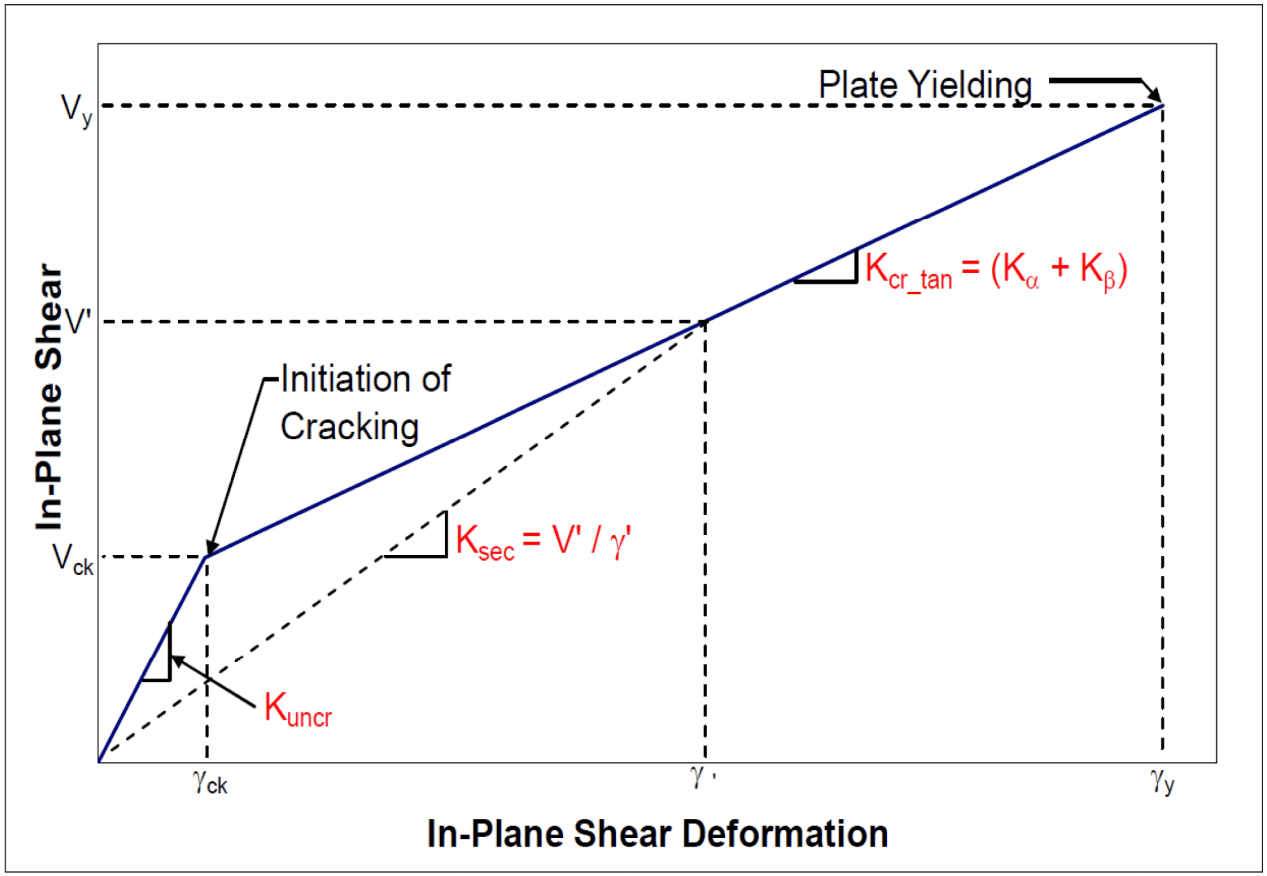

Figure 4-3 Bilinear Shear-Deformation Relationship for SC Walls

Figure 4-4 Secant Stiffness vs. In-Plane Shear Force for Category 1 SC Walls
The plot shows the range of normalized reinforcement ratios used in the US-APWR CIS.

Figure 4-5 Comparison of Equation 4-10 vs. Fully Cracked Secant Stiffness
For the typical 48”-thick Category 1 SC wall geometry with ½”-thick faceplates.

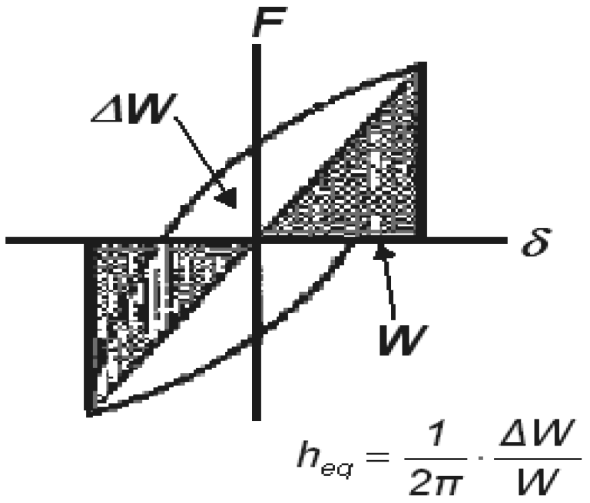

Figure 4-6 Equivalent Viscous Damping from Hysteretic Loop
(As given in Reference 21).

Member	Flexural Rigidity	Shear Rigidity	Axial Rigidity
Walls and Diaphragms--Uncracked	$E_c I_g$	$G_c A_w$	$E_c A_g$
	$(f_b < f_{cr})$	$(V<V_c)$	
Walls and Diaphragms--Cracked	$0.5E_c I_g$	$0.5G_c A_w$	$E_c A_g$
	$(f_b > f_{cr})$	$(V>V_c)$	

Notes:

A_g = Gross Area of the Concrete Section

A_w = Web Area

E_c = Concrete Compressive Modulus

G_c = Concrete Shear Modulus = 0.4 E_c

f_b = Bending Stress

f_{cr} = Cracking Stress

V = Wall Shear

V_c = Nominal Concrete Shear Capacity

Table 4-1 Effective Stiffness Values for RC Walls and Slabs
As given in ASCE 43-05 (Reference 23).

5.0 EVALUATION OF STIFFNESS AND DAMPING FOR LOADING CONDITION "A"

As discussed in Section 3, the normal operating temperatures are not expected to cause significant cracking in any of the CIS structure categories. Thus the extent of cracking for Condition "A" may be reasonably estimated by evaluating stresses resulting from SSE loading only.

To facilitate this evaluation, response spectrum analysis was performed using the detailed ANSYS model prepared for basic design of the CIS (Reference 11). For this evaluation, the analysis model used uncracked (full) stiffness values. The inputs to the analysis were three translational acceleration response spectra generated at the base of the CIS in the SSI analysis of the reactor building (R/B) complex described in Reference 13. In accordance with Regulatory Guide 1.92 (see Reference 19), the Lindley-Yow method was used to separate the rigid and periodic responses of the CIS for each direction of motion, and the periodic responses were combined using the Complete Quadratic Combination (CQC) method. The rigid response was then calculated using the static zero-period acceleration (ZPA) method, and the periodic and rigid responses were combined by square-root-sum-of-the-squares (SRSS); i.e. Combination Method "B" was used. The hydrodynamic response of the refueling water in the RWSP was also included in each of the directional response components, as described in Reference 11. Finally, the three directional response components were combined by SRSS and added to the absolute value of the accidental torsion load case to obtain a total seismic load case representing the maximum earthquake-induced response of the CIS.

The paragraphs below present the evaluation of cracking and associated stiffness reductions that were performed for each of the structure categories using the initial seismic analysis. The evaluations are presented in the given order to simplify explanation of the approaches taken. The results of these evaluations are summarized in Section 7 and in the list of stiffness and damping values given in Table 7-1.

5.1 Category 1 In-Plane Shear Stiffness Evaluation

The following procedure was applied to determine appropriate values for the in-plane shear stiffness of the Category 1 SC walls under Condition "A":

1. *Group the SC wall elements in the model into collections of elements that form individual walls in the structure*. This procedure was performed in ANSYS using element "components," which can contain any selected set of elements and can be given an appropriate name. The SC wall components were generally selected such that all elements in the component may be considered to act together as a wall that transfers in-plane shear from one floor to another in a given direction. Thus the components include elements with common cross-sectional properties and typically have boundary conditions comprised of a slab or mat at the bottom edge, a slab at the top edge, and transverse walls at either end. The ANSYS plot in Figure 5-1 shows one example of the 96 components defined in this fashion.

2. *Calculate the uncracked in-plane shear stiffness for each wall component geometry*, using Equation 4-1.

3. *Extract the seismic in-plane shear forces on each wall component and calculate the secant stiffness for the wall*. In order to automate this procedure, a routine was written in ANSYS that assumed the overall shear applied at the top of the wall is

distributed to the elements of the wall on a per-foot basis. This assumption was deemed reasonable for the manner in which the elements were grouped in step 1, and was subsequently verified by hand calculations that considered the wall as a whole. The ANSYS routine extracted the seismic in-plane shear force on each element and calculated the element secant stiffness using the bilinear shear deformation curve as described in Section 4.1.3. The element secant stiffnesses were then averaged to obtain the secant stiffness of the wall.

4. *Compute the ratio of secant stiffness to uncracked stiffness* using the results of steps 2 and 3.

5. *Compute the ratio of effective stiffness to uncracked stiffness* using Equation 4-12, recalling that the initial stiffness is considered the uncracked stiffness for Condition "A".

The results of this procedure are shown in Table 5-1. The calculated effective stiffness values are shown to be close or equal to the uncracked stiffness for a majority of the SC walls, which indicates that the seismic in-plane shear demands are relatively low for the thick wall geometries provided in the CIS. In accordance with the third objective stated in Section 1.2, the tabulated results support the use of the composite uncracked in-plane shear stiffness for all of the Category 1 walls under Condition "A", recognizing that the cracked in-plane shear stiffness is to be used for Condition "B" (as will be discussed further in Section 6). This approach will capture the reduced stiffness values calculated for some of the walls in the present evaluation.

As mentioned in Section 4.1, the out-of-plane flexural stiffness for the Category 1 SC walls is taken as that of the cracked-transformed section for all loading conditions. Since the in-plane shear stiffness of these walls has a more significant impact on the CIS dynamic response, the uncracked damping ratio of 4% discussed in Section 4.1.7 is considered appropriate for the Category 1 walls under Condition "A".

5.2 Category 4 Out-of-Plane Flexural Stiffness Evaluation

The primary dynamic response of interest for the Category 4 floor slabs is their out-of-plane (vertical) response. Thus the results of the initial seismic analysis were also used to evaluate the extent of out-of-plane flexural cracking in each of the major floor slabs. The following procedure was applied to determine appropriate stiffness values for the Condition "A" analyses, in accordance with ASCE 43-05 (Reference 23):

1. *Group the RC slab elements in the ANSYS model into components*. Five major reinforced concrete slabs were identified in the CIS structure, including slabs at top-of-concrete elevations 25'-3", 37'-9", 50'-2", 76'-5", and 139'-6". The locations of these slabs are shown in Figures 2-1 through 2-7.

2. *Combine the total seismic case with dead load to create two load cases*: *Dead Load + Seismic Load, and Dead Load - Seismic Load*. These two cases must be considered to include the flexural stresses due to the structure dead load and because the signs of the seismic stress resultants are lost in the SRSS procedures discussed above.

3. *For each element in a given slab, extract the out-of-plane moments MX, MY, and MXY for each of the two loading conditions.*

4. *Calculate the maximum principal moments in each element, for each loading condition.* The following formulas are used:

(Equation 5-1) $$M_1, M_2 = \frac{MX + MY}{2} \pm \sqrt{\left(\frac{MX - MY}{2}\right)^2 + MXY^2}$$

(Equation 5-2) $$M_{max} = max\left(|M_1|, |M_2|\right)$$

5. *Calculate the cracking moment for each slab geometry,* using the formulas provided in ACI 349-01 Section 9.5.2.3 (Reference 9):

(Equation 5-3) $$M_{cr} = \frac{f_r I_g}{y_t}$$

(Equation 5-4) $$f_r = 7.5 \cdot \sqrt{f'_c}$$

where f_r is the modulus of rupture of concrete, I_g is the moment of inertia of the gross section per unit width, and y_t is half the thickness of the gross section.

6. *Compare the maximum principal moments in each element (from either load case) to the cracking moment, and calculate the percentage of elements that are cracked.*

The results of this procedure are shown in Table 5-2. The computed maximum principal moments are shown to be less than the cracking moment for most of the elements in each of the five major slabs. The slab with the most elements cracked in flexure is the operating floor at Elevation 76'-5", in which 12% of the elements are cracked. The ANSYS contour plot shown in Figure 5-2 indicates that flexural cracking in this slab is limited to the region immediately adjacent to the secondary shield walls to which the slab is rigidly connected. Since most of the elements in each of the major slabs are uncracked, a bounding approach similar to that described for in-plane shear stiffness of the Category 1 walls is to be used for the RC slabs: the uncracked out-of-plane flexural stiffness is to be used for Condition “A”, recognizing that the cracked stiffness is to be used for Condition “B”. This will ensure that any modification of dynamic response due to flexural cracking is sufficiently covered in the enveloped results.

The Category 4 slabs do not carry significant in-plane shear forces under seismic loading. Thus the uncracked in-plane shear stiffness is assigned to the slabs for Condition “A”. Given that both the flexural and in-plane shear stiffness of the slabs are considered uncracked for this condition, a 4% damping ratio is assigned in accordance with the intent of Regulatory Guide 1.61 (Reference 4).

5.3 Evaluation of Concrete Stresses in Categories 2, 3, and 5

5.3.1 Category 2 Walls

As discussed in Section 4.2, the Category 2 walls are treated as reinforced concrete structures in terms of their stiffness and damping characteristics. In accordance with ASCE 43-05 (Reference 23), the in-plane shear stiffness of these walls was evaluated for Condition “A” by

determining the extent to which the applied seismic in-plane shear forces exceed the concrete in-plane shear strength, which is given in ACI 349-01 Section 21.6.5 (Reference 9) as:

(Equation 5-5) $$V_c = A_{cv}(2\sqrt{f'_c})$$

where A_{cv} is the cross-sectional area of the wall in the direction of the applied shear force.

Figure 5-3 presents an ANSYS contour plot of the seismic in-plane shear forces (NXY) applied to the Category 2 walls that were modeled with shell elements, which includes the 67"-thick walls in the refueling canal area (this comprises a majority of the Category 2 walls). As shown in the plot, the in-plane shear forces in excess of the concrete shear strength are limited to a small portion of the walls. Therefore the uncracked in-plane shear stiffness is warranted for use with Condition "A", given that the cracked stiffness is to be used for Condition "B". It is noted that the stiffness considered will be that of the concrete section only, as is customary for reinforced concrete sections.

To evaluate the out-of-plane flexural stiffness of these walls, a procedure similar to that used for the reinforced concrete slabs was applied. Figure 5-4 shows that the seismically induced maximum principal moments for the elements of the Category 2 walls were in all cases less than the cracking moment. Thus the uncracked out-of-plane flexural stiffness given for RC sections is to be used for Condition "A".

Given that these walls are considered uncracked for both in-plane shear and flexural stiffness, they are assigned a damping ratio of 4% for Condition "A", in accordance with the intent of Regulatory Guide 1.61 (Reference 4).

5.3.2 Categories 3 and 5

The Category 3 and 5 structures in the CIS are also treated as reinforced concrete when evaluating the effects of cracking on their stiffness and damping properties. The Category 3 primary shield walls are not anticipated to experience seismically induced in-plane shears or out-of-plane moments beyond the cracking threshold, given their large cross-sectional thickness, their rigid cylindrical arrangement, and the fact that they are confined by the Category 5 massive reinforced concrete over much of their height (see Figures 2-6 and 2-7). Likewise, the Category 5 sections themselves are not expected to experience seismically-induced cracking in light of their rigid geometries.

Both of these structure categories were modeled in ANSYS with three-dimensional solid elements. Thus it is necessary to evaluate the stated assumption of limited stresses under seismic loading by comparing maximum principal stresses to the tensile strength of concrete. Figures 5-5 and 5-6 present ANSYS contour plots for the Category 3 and Category 5 structures, respectively, of maximum principal stress due to a load case consisting of dead load plus total seismic load. This case is considered because the signs of component stresses in the total seismic load case are all positive, such that the addition of the seismic load case to dead load maximizes tensile principal stresses in the output, while the dead load minus seismic load case results in more compressive principal stresses. As shown in the figures, principal stresses in excess of the tensile strength of concrete (taken as $4\sqrt{f'_c}$) are limited to small portions of both the Category 3 and Category 5 elements in the model. Therefore these structures are assigned uncracked RC stiffness and damping values for Condition "A".

Figure 5-1 CIS ANSYS Model Showing Wall Component Selection

Figure 5-2 Maximum Slab Principal Moments Due to Seismic Loading
ANSYS contour plot of maximum principal moments calculated for the elements of the slab at top-of-concrete elevation 76'-5". Contour intervals are set such that green through red elements have moments in excess of the cracking moment (M_{cr}).

Figure 5-3 Seismic In-Plane Shear Forces in Category 2 Walls
ANSYS contour plot of in-plane shear forces in the 67"-thick walls in the refueling canal area. Contour intervals are set such that red elements have in-plane shear forces (NXY) in excess of the concrete capacity (V_c).

Figure 5-4 Max. Principal Moments in Category 2 Walls Due to Seismic Loading
ANSYS contour plot of maximum principal moments calculated for the elements of the Category 2 walls in the refueling canal area. The cracking moment (M_{cr}) is not exceeded in any element.

Figure 5-5 Max. Principal Stresses in Category 3 Walls Due to Seismic Loading
ANSYS contour plot of maximum principal stresses calculated for the Category 3 Primary Shield walls. Stresses in excess of the concrete tensile strength are limited to small areas, primarily in the vicinity of the RCL connection points.

Figure 5-6 Max. Principal Stresses in Category 5 Structures Due to Seismic Loading
ANSYS contour plot of maximum principal stresses calculated for the Category 5 Structures. Stresses in excess of the concrete tensile strength are limited to small areas.

Table 5-1 Summary of Effective In-Plane Shear Stiffness Ratios
For Loading Condition “A”.

Table 5-2 Summary of RC Slab Flexural Cracking Evaluation
For Loading Condition “A”.

6.0 EVALUATION OF STIFFNESS AND DAMPING FOR LOADING CONDITION "B"

The evaluation of seismically induced concrete stresses discussed in Section 5 rendered the assessment that all of the structure categories in the CIS are largely uncracked for Condition "A". As discussed in Section 3, the addition of accident thermal loading is anticipated to result in significant concrete cracking of the various walls and slabs of the CIS.

6.1 Heat Transfer Analysis

When the accident thermal temperatures shown in Figure 3-1 occur in the compartments of the CIS, nonlinear temperature gradients will form through the thickness of the walls. In order to determine the magnitude and distribution of these temperature gradients with respect to time, heat transfer analyses were performed in support of the CIS basic design (Reference 11). These analyses utilized a finite difference approach wherein one-dimensional conduction was assumed through the thickness of the wall; i.e. the in-plane extents of the wall were considered infinite and uniform surface temperatures were assumed. The analyses also assumed that the steel faceplates on the walls directly conduct the ambient compartment temperatures to the faces of the concrete core, and that the concrete material properties are constant and isotropic.

Figure 6-1 shows the heat transfer analysis results for the 48"-thick Category 1 SC walls that are used extensively in the CIS. The plot illustrates that steep, parabolic temperature gradients are formed initially through the thickness of the section, and that these gradients gradually decrease with time as heat is conducted into the concrete core. In terms of concrete cracking, these temperature gradients are anticipated to have two major effects. First, the steep initial gradients are expected to induce high in-plane tensile stresses in the concrete core that will result in through-thickness cracking. Second, the net increase of the wall temperatures from the baseline operating temperatures are expected to cause significant growth of the overall section. The restraint of this growth at supports, corners, and other structural discontinuities is expected to induce significant out-of-plane moments that may potentially cause flexural cracking.

6.2 Category 1 Stiffness Evaluation

To evaluate the in-plane stresses induced by the initial temperature gradients observed in the heat transfer analysis, a linear thermal stress analysis was conducted in ANSYS that considered the temperature gradient at 1000 seconds on the typical 48"-thick SC wall section. As shown in Figure 6-2, a three-dimensional model of a wall section was generated that utilized solid elements for the concrete core and shell elements for the steel faceplates. The 1000-second temperatures were then applied to the nodes to create the gradient, and boundary conditions were applied that permitted thermal expansion both in and out of the plane of the wall.

The results of this analysis are presented in Figure 6-3. The figure shows a sectional view of the concrete core in which the variation of vertical in-plane stresses through the thickness of the concrete can be seen. It is observed that the parabolic thermal gradient puts the outer fibers of the concrete core into compression, while the central portion of the concrete thickness is put into tension. The plot contours indicate that the tensile stresses greatly exceed the concrete tensile strength (taken as $4\sqrt{f'_c}$) over the majority of the section. Thus it can be postulated that in the actual, nonlinear structure, the accident condition temperature gradients would result in through-thickness cracks at intervals along the length and height of the wall.

As illustrated in Appendix D, experiments performed in Japan have demonstrated that the accident thermal condition does cause thermal gradients similar to those predicted by the aforementioned heat transfer analysis, and that the gradients cause the postulated through-thickness cracking in two orthogonal directions. Importantly, these tests also evaluated the reduction in in-plane shear stiffness of SC sections caused by the thermally-induced cracking. As explained in Appendix D, the results indicated that the tangent in-plane shear stiffness under all applied shear forces was approximately equal to the post-cracking shear stiffness of the composite section, i.e. $K_s + K_{sc}$ as given above by Equation 4-4. Therefore the secant stiffness for the accident thermal condition may be estimated as that of the fully cracked section, as given by Equation 4-10.

Recalling that the out-of-plane flexural stiffness for composite SC walls is taken as that of the cracked-transformed section for all loading conditions, the Category 1 walls are considered cracked for Condition “B” in both shear and flexure. As a result, the cracked damping ratio of 5% discussed in Section 4.1.7 is appropriate for Category 1 under this condition.

6.3 Category 2 Stiffness Evaluation

The in-plane cracking observed in the analysis and experiments for the Category 1 SC walls is also anticipated for the Category 2 walls, which are exposed to the same ambient compartment temperatures during the accident condition. The Category 2 walls will also experience steep parabolic temperature gradients that result in extensive through-thickness concrete cracking. In accordance with ACI 349.1R Section 1.4 (see Reference 25), the effect of this cracking may be addressed in linear elastic analysis models of RC structures by reducing the concrete modulus of elasticity by 50%. This reduction is consistent with that specified in ASCE 43-05 (Reference 23) for cracked in-plane shear stiffness of RC walls. It is also comparable to the reduction in secant stiffness applied to the Category 1 SC walls for this condition, as will be further discussed in Section 8.

Flexural stresses induced by thermal loading in the various walls and slabs of the CIS were evaluated using the analysis of the accident thermal condition that was performed in support of the basic design (Reference 11). The intent of this analysis was to assess the stresses induced by restraint of overall thermal growth of the structure. Thus, the average increase in wall and slab temperatures at a given point in time, as given by the heat transfer analysis results specific to each member thickness, were applied to each component of the structure. The point in time considered in this analysis was selected as the point at which the average temperature of the 48”-thick SC walls was maximized, since these walls comprise a majority of the walls in the structure. This was calculated to occur at four days after the postulated pipe rupture, using the thermal gradients given in Figure 6-1.

The results of this analysis were combined with seismic loading and used to evaluate the extent of out-of-plane flexural cracking in the Category 2 walls for Condition “B”. The procedure for this evaluation was similar to that used for Condition “A”; i.e. principal moments due to the Condition “B” loading were compared to the cracking moment for the section (calculated using Equations 5-3 and 5-4). The principal moment contour plot given in Figure 6-4 indicates that, as was expected, moments in excess of the cracking moment occur at the base of the walls and at other discontinuities. The presence of significant cracking for this condition warrants the previously mentioned bounding approach for Category 2 flexural stiffness, wherein the uncracked stiffness is assigned for Condition “A” and the cracked stiffness is assigned for Condition “B”.

Since both cracked in-plane shear stiffness and cracked out-of-plane flexural stiffness are to be assigned for the Category 2 walls, a damping ratio of 7% is considered appropriate for these walls under Condition “B”. This is in accordance with the guidance provided in Regulatory Guide 1.61 for reinforced concrete walls (Reference 4).

6.4 Category 3 Stiffness Evaluation

The Category 3 primary shield walls are irregular in terms of both their geometry and their exposure to thermal loading. As such, evaluation of the response of these walls to accident thermal loading is not straightforward. In terms of geometry, the walls are arranged in a very rigid, cylindrical shape with nominal thickness that varies from 10 feet to 15 feet. In addition, the walls have an array of transverse and mid-thickness longitudinal steel plates that divide the concrete into numerous cells, and the walls have four large penetrations for fuel loading instrumentation and equipment. In terms of exposure to thermal loading, Figures 2-6 and 2-7 illustrate that the primary shield walls are encapsulated by the Category 5 massive reinforced concrete over more than half of their overall height. The Category 5 concrete not only prevents exposure of the outer primary shield face to accident temperatures, but it also restrains any thermal growth of the primary shield walls. Above the Category 5 concrete, the primary shield walls are also restrained on all sides by six different secondary shield walls that frame into the outer primary shield face (see Figure 2-2) and by the reinforced concrete slabs at elevations 25'-3" and 37'-9" (see Figure 2-6).

Clearly the conditions assumed by the heat transfer analyses discussed for the Category 1 and 2 walls are not at all applicable to the Category 3 walls. In order to accurately assess the extent of cracking and attendant stiffness reductions induced in these walls by the Condition “B” loading, a detailed transient thermal analysis would be required, followed by application of seismic loading. This analysis has not been performed to date. Nevertheless, it is deemed a reasonable assumption that the walls will remain largely uncracked for this condition, given the low stress exhibited for seismic loading alone, the minimal exposure of the outer face of the walls to thermal loading, and the relatively uniform restraint of thermal growth applied by the surrounding structures. The assumption of minimal cracking and reduction of stiffness for this condition will be reevaluated and verified as the CIS design progresses.

6.5 Category 4 Stiffness Evaluation

The Category 4 reinforced concrete slabs are generally exposed on both faces to the accident thermal temperatures shown in Figure 3-1. As such, their response to thermal loading is assessed using the thermal analysis performed on the CIS for the basic design, as discussed above for the Category 2 walls. Principal moments were calculated for each of the major slabs in the CIS under the 4-day accident thermal condition combined with seismic and dead loads, and then compared to cracking moments calculated using Equations 5-3 and 5-4.

Figure 6-5 shows the results of this evaluation for the slab at Elevation 25'-3". This slab is primarily 40" thick, with 51" thickness in certain areas as shown in the figure. The slab is shown to experience significant thermally induced flexure due to its rigid connection to both the outer RWSP wall and the secondary shielding walls. It is noted from the contours given in the figure that the calculated principal moments exceed the cracking moment in a majority of the slab elements. The presence of significant out-of-plane cracking under this condition justifies use of cracked flexural stiffness and 7% damping for the Category 4 slabs under Condition “B”. This establishes a bounding analysis approach for the primary dynamic response of interest for these slabs, given that uncracked flexural stiffness and 4% damping is to be used for Condition “A”.

6.6 Category 5 Stiffness Evaluation

As shown in Figures 2-6 and 2-7, the massive reinforced concrete sections in the CIS are founded on the thick R/B complex mat. As a result, exposure to elevated temperatures following a postulated pipe rupture is generally limited to the top faces and some of the vertical inside faces of these structures. Since all of the Category 5 structures are extremely thick (both horizontally and vertically), this limited exposure to the accident temperatures is not expected to cause significant reductions of stiffness due to concrete cracking. Therefore uncracked stiffness and damping values are considered the best estimate for Category 5 under Condition “B”.

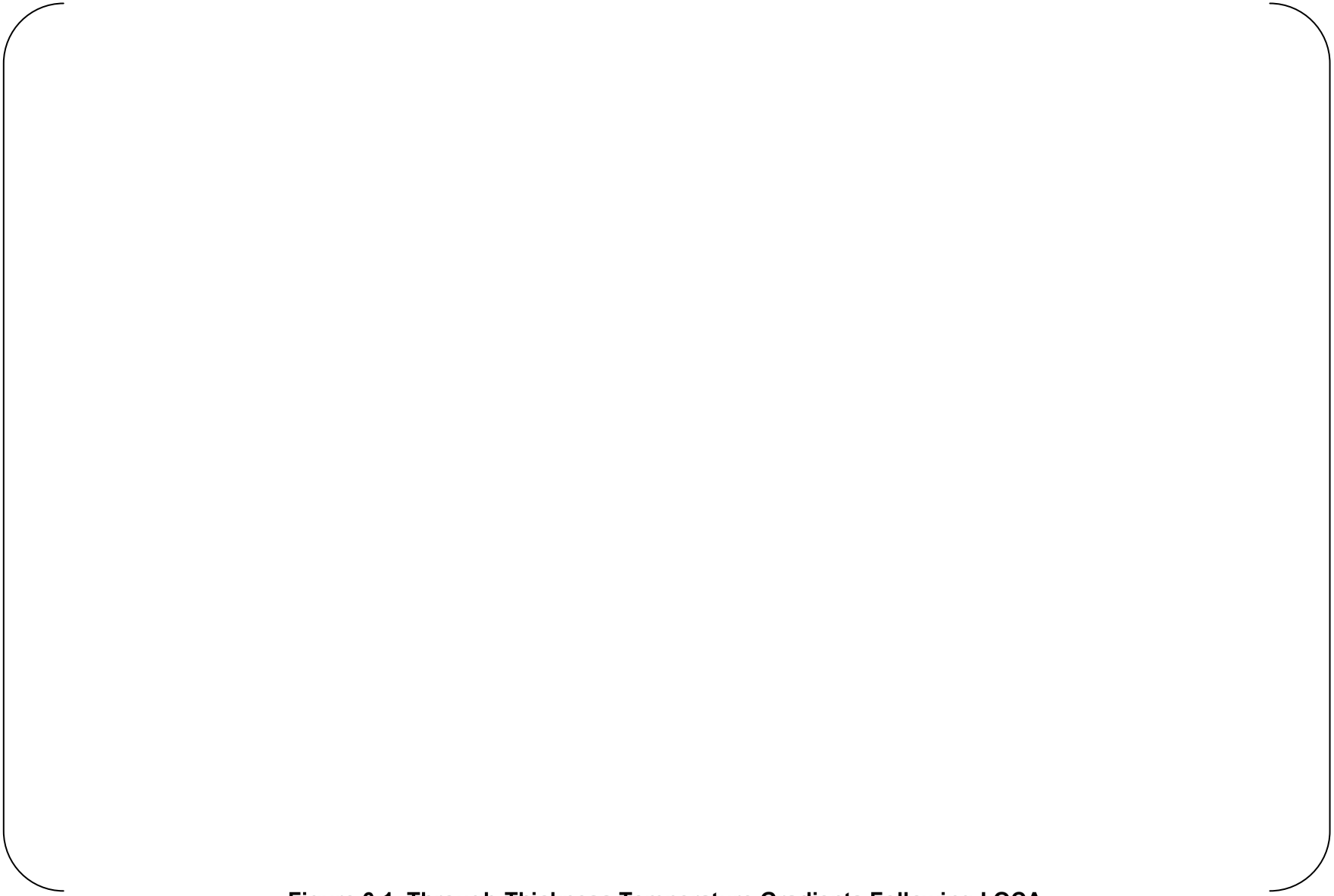

Figure 6-1 Through-Thickness Temperature Gradients Following LOCA
Temperature gradients for the 4'-0"-thick SC walls are shown for various timeframes.

Figure 6-2 ANSYS Model for Analysis of Accident Thermal Stress in SC Walls

Figure 6-3 In-Plane (Vertical) Stresses Due to Accident Thermal Temperature Gradient

Figure 6-4 Max. Principal Moments in Category 2 Walls for Condition "B"
ANSYS contour plot of maximum principal moments calculated for the elements of the Category 2 walls in the refueling canal area.

Figure 6-5 Max. Principal Moments in Slab @ Elev. 25'-3" for Condition "B"
It is noted that the slab consists of two thicknesses, for which corresponding cracking moments are calculated and used to define the contour intervals.

7.0 SUMMARY OF STIFFNESS AND DAMPING VALUES FOR ANALYSIS

A summary of the stiffness and damping values defined above is provided in Table 7-1. For each of the six major structure categories, the table presents the in-plane shear stiffness, out-of-plane flexural stiffness, and damping ratios that have been deemed appropriate for the two analysis cases (Condition “A” and Condition “B”). In general, the table shows that the structure is to be considered as largely uncracked for Condition “A” and cracked for Condition “B”. In several cases, the tabulated values reflect the decision to apply a bounding approach when the assessment of stresses indicated the given structure category was mostly uncracked for Condition “A” and significantly cracked under Condition “B”. Such is the case for the in-plane stiffness of the Category 1 and Category 2 walls and for the flexural stiffness of the Category 4 slabs. However, a bounding analysis approach was not imposed for all structure categories, in the interest of obtaining realistic dynamic responses from both the Condition “A” and Condition “B” analyses. For example, both the Category 3 and Category 5 structures are anticipated to remain mostly uncracked under either loading condition and so a bounding approach is not warranted for these structures. Likewise, the flexural stiffness of the Category 1 SC structures is best approximated by the cracked-transformed stiffness under either loading condition.

In terms of damping, the category-specific damping ratios provided in the table could be applied to each of the various structures in the CIS for each of the two dynamic analyses. However, examination of the individual values given in the table suggests that constant damping ratios may be used. For Condition “A”, 4% damping is identified for all of the structure categories, such that 4% damping is clearly appropriate as an overall, constant damping ratio. For Condition “B”, the individual values range from 4% for the uncracked reinforced concrete structures to 7% for the cracked reinforced concrete structures, with 5% assigned to the Category 1 SC walls. Since the Category 1 walls are the primary lateral load resisting members in the structure and their response dominates the amplified range of the overall structure response, 5% damping is deemed an appropriate constant damping ratio for the Condition “B” analyses. In accordance with the guidance given in Regulatory Guide 1.61 (Reference 4), this value is considered appropriate both for generation of forces for structural design and for generation of in-structure response spectra for equipment design, since it represents the best estimate of energy dissipation with the cracking levels identified for this condition. It is noted that the 5% value is somewhat conservative for the cracked reinforced concrete slabs and the cracked Category 2 walls. Damping is not expected to have a significant impact on the seismic response of the relatively rigid structures of Categories 3 and 5, regardless of the values assigned to these structures.

Structure Category	Description	Loading Condition A ($E_{ss} + T_o$)			Loading Condition B ($E_{ss} + T_a$)		
		Shear Stiffness	Flexural Stiffness	Damping	Shear Stiffness	Flexural Stiffness	Damping
1	SC Walls, T≤ 56"	Uncracked $G_cA_c + G_sA_s$	Cracked-Transformed E_cI_{ct}	4%	Fully Cracked $0.5\ (\rho^{-0.42})A_sG_s$	Cracked-Transformed E_cI_{ct}	5%
2	Walls with T> 56"	Uncracked RC G_cA_c	Uncracked RC E_cI_c	4%	Cracked RC $0.5\ G_cA_c$	Cracked RC $0.5\ E_cI_c$	7%
3	Primary Shielding	Uncracked RC G_cA_c	Uncracked RC E_cI_c	4%	Uncracked RC G_cA_c	Uncracked RC E_cI_c	4%
4	RC Slabs	Uncracked RC G_cA_c	Uncracked RC E_cI_c	4%	Uncracked RC G_cA_c	Cracked RC $0.5\ E_cI_c$	7%
5	Massive RC Sections	Uncracked RC G_cA_c	Uncracked RC E_cI_c	4%	Uncracked RC G_cA_c	Uncracked RC E_cI_c	4%
6	Steel Structure with Nonstructural Concrete Infill	No Concrete Stiffness or Damping Applied					

Table 7-1 Summary of CIS Stiffness and Damping Values

8.0 APPLICATION

As mentioned previously, the dynamic response of the CIS will be analyzed using 3-D LEFE models. These models explicitly account for the 3-D geometry of the structure including the extents of each individual wall and slab, using finite elements with linear elastic, isotropic material properties. Thus the geometry of each wall and slab will be modeled using either 3-D solid elements or shell elements. The linear elastic material properties (elastic modulus E and Poisson's ratio ν) and the thickness (t) of these elements will be calibrated to match the effective in-plane shear stiffness and out-of-plane flexural stiffness values given for each structure category in Table 7-1. As stated in the fourth objective in Section 1.1, the calibrated properties will be assigned consistently to the elements of both the ACS SASSI dynamic FE model and the ANSYS detailed design FE model. The primary purpose of this section is to illustrate the manner in which these material and section properties are calculated. In addition, the axial stiffness terms that result from this calibration approach are evaluated, and finally the complete set of stiffness values assigned to the Category 1 SC structures are compared to those recommended in the available nuclear standards for RC structures.

8.1 Calculation of Equivalent Material Properties for Category 1 Walls

The analysis models for both the SSI analysis and the detailed design will use single-layer shell elements with isotropic material properties to model the composite Category 1 SC walls. The procedure presented below is used to calculate equivalent values of section thickness (t') and elastic modulus (E') to match the composite in-plane shear and out-of-plane flexural stiffness values given in Table 7-1.

1. Calculate the in-plane shear stiffness of the section using Equation 4-1 for Condition "A" or Equation 4-10 for Condition "B":

   (Equation 4-1) $$GA_{uncr} = K_{uncr} = G_c A_c + G_s A_s$$

   (Equation 4-10) $$GA_{cr} = K_{cr} = 0.5\left(\rho^{-0.42}\right) G_s A_s$$

2. For both Conditions "A" and "B", calculate the cracked transformed flexural stiffness for the section using Equation 4-13:

   (Equation 4-13) $$EI_{cr\_tr} = E_s I_s + \alpha E_c I_c$$

3. Setting $EI = \left(E \cdot t^3\right)/12$, $GA = \left(E \cdot t\right)/[2(1+\upsilon)]$ and $\nu = \nu_c$, solve two equations and two unknowns to obtain E' and t' that provide the correct values for *GA* and *EI* calculated in steps 1 and 2:

   (Equation 8-1) $$t' = \sqrt{\frac{12EI_{cr\_tr}}{2(1+\nu_c)(GA_{uncr} \text{ or } GA_{cr})}}$$

   (Equation 8-2) $$E' = \frac{2(1+\nu_c)(GA_{uncr} \text{ or } GA_{cr})}{1in \cdot t'}.$$

4. Calculate the equivalent density to maintain the correct unit weight with the calculated equivalent thickness:

(Equation 8-3) $$\rho' = \frac{\left(A_c \cdot \rho_c + A_s \cdot \rho_s\right)}{1in \cdot t'}$$

Appendix G provides the complete set of calculations that follow this procedure for each of the Category 1 wall geometries. The appendix also provides property calculations for all other structure categories in the CIS for input to the analysis models.

8.2 Discussion of associated axial stiffness

As mentioned in Section 4.1.6, the Category 1 SC wall axial stiffness values implicitly obtained with the E' and t' values calculated in the manner described above must be evaluated for each of the two loading conditions. The equivalent axial stiffness is calculated per unit width as:

(Equation 8-4) $$(EA)' = E' \cdot t'$$

For the upper bound stiffness of Condition "A", the equivalent axial stiffness is evaluated by comparing it to the actual uncracked composite stiffness, which is calculated as follows:

(Equation 8-5) $$EA_{uncr} = E_s A_s + E_c A_c$$

For the lower bound stiffness of Condition "B", the equivalent axial stiffness is compared to the average of cracked and uncracked composite axial stiffnesses, defined previously in Equation 4-16:

(Equation 4-16) $$EA_{avg} = \frac{1}{2}\left[E_s A_s + \left(E_s A_s + E_c A_c\right)\right] = E_s A_s + \frac{E_c A_c}{2}$$

These comparisons are performed in the calculations given in Appendix G. The axial stiffness terms calculated with the equivalent material and section properties for Condition "A" are shown to be within 2.6% of the actual uncracked stiffness for all of the Category 1 wall geometries. For Condition "B", the equivalent properties render axial stiffness values that are somewhat softer than the average of the cracked and uncracked composite stiffnesses given by Equation 4-16; the equivalent values range between 60% and 76% of the average values. In light of the extensive through-thickness cracking anticipated for Condition "B", these equivalent axial stiffness values provide a rational lower bound for the Category 1 walls. This assessment is further confirmed in view of the axial stiffness values prescribed for RC walls under accident thermal conditions, as discussed below.

8.3 Comparison of SC and RC Stiffness Values

Table 8-1 compares stiffness values for the common 48-in. thick SC wall with 0.5-in. thick steel faceplates computed using the equations in Section 4 for SC walls with those prescribed by current nuclear standards for RC structures. Specifically, ASCE 43-05 Table 3-1 (Reference 23) is considered for stiffness values of RC structures under seismic loading during normal operations (Condition "A") and ACI 349.1R (Reference 25) is considered for stiffness reductions due to accident thermal loading (Condition "B"). The various in-plane

shear, out-of-plane flexural, and axial stiffness values tabulated for each condition are calculated in Appendix G.

In general, the comparison in Table 8-1 illustrates that the SC-specific formulations for stiffness result in values that are not substantially different from those codified for RC structures. It must be noted, however, that this close comparison is primarily a function of the particular reinforcement ratios selected for the US-APWR Category 1 SC walls. As discussed in Section 4 and the appendices, the tabulated SC stiffness values reflect the behavior of the continuous SC faceplates acting compositely with the concrete core to resist in-plane and out-of-plane loads. This behavior is significantly different than that of concrete reinforced with an orthogonal grid of reinforcement. Nevertheless the favorable comparison of SC and RC stiffness values does indicate that the dynamic response of the US-APWR CIS will be similar to that of a containment internal structure constructed entirely of reinforced concrete. The reasonably small differences in each stiffness term are readily explained in terms of SC vs. RC behavior.

For Condition “A”, the SC-specific axial and in-plane shear stiffness terms are shown to be 13% larger than those of uncracked reinforced concrete. Again, this difference is the result of composite resistance to in-plane loads of the steel and concrete in SC construction, while the magnitude of the difference is a function of the selected reinforcement ratio (2.1% in this case). The SC-specific flexural stiffness term for Condition “A” is 63% of that obtained with the RC equation. This difference reflects the fact that SC wall out-of-plane flexural stiffness is best approximated as the cracked-transformed stiffness, as discussed in Appendix E.

For Condition “B”, the SC-specific stiffness values are compared to those obtained using $0.5E_c$, as recommended in ACI 349.1R Section 1.4 for linear elastic analysis of RC structures with thermally induced cracking. For in-plane shear stiffness and axial stiffness, the SC-specific values are 84% of the cracked stiffness values calculated with the RC equations ($0.5G_cA_g$ and $0.5E_cA_g$, respectively). Once again the values are similar, but the SC-specific values reflect the larger in-plane stiffness reduction anticipated for the extensive cracking caused by accident thermal loading, which has been experimentally verified (see Appendix D.) While it is acknowledged that the SC-specific axial stiffness value is likely too soft for portions of walls in compression during seismic loading, it is nevertheless considered a rational lower bound case for use in linear elastic analyses. Any differences in dynamic response due to higher axial stiffness will be captured with the uncracked axial stiffness assigned for Condition “A”. The SC-specific out-of-plane flexural stiffness for this condition is somewhat higher than the value computed for RC, which simply reflects the composite cracked-transformed flexural stiffness for the particular reinforcement ratios used in the US-APWR CIS.

Table 8-1 Comparison of SC and RC Stiffness Values
Stiffness values for the common 48”-thick SC wall section are computed using the SC-specific equations in Section 4 and the RC equations given in ASCE 43-05 (Reference 23) for Condition “A” and ACI 349.1R (Reference 25) for Condition “B”.

9.0 SUMMARY

An accurate dynamic analysis can only be performed with a linear elastic model if the model uses the best possible estimation of the effective elastic constants. To this end, stiffness values for each of the structure categories in the CIS have been calculated based on the formulations outlined in Section 4, and in consideration of the extent of concrete cracking caused by seismic and accident thermal loading. Two sets of stiffness and damping values have been calculated that capture the potential range of stresses and associated cracking levels in each structure category. It has been shown that both sets of stiffness values obtained with formulations specific to the composite behavior of the Category 1 SC walls are reasonably close to those of RC walls. The manner in which the two sets of stiffness values are applied to the linear elastic models for SSI analysis and detailed structural design has been illustrated. Two corresponding sets of analyses will be conducted in both ACS SASSI and ANSYS to complete Tasks 1-A and 1-B, respectively, in the overall CIS design and validation plan. The enveloped results from these analyses will provide a conservative assessment of the potential range of demands for which the CIS structures and equipment must be designed.

10.0 REFERENCES

1. Mitsubishi Heavy Industries, Ltd., *"Containment Internal Structure Design and Validation Methodology"*, MUAP-11013, Revision 1, August 2011.
2. Mitsubishi Heavy Industries, Ltd., *"Soil-Structure Interaction Analyses and Results for the US-APWR Standard Plant"*, MUAP-11001, Revision 1, July 2011.
3. Mitsubishi Heavy Industries, Ltd., *"Research Achievements of SC Structure and Strength Evaluation of US-APWR SC Structure Based on 1/10th Scale Test Results"*, MUAP-11005, Revision 0, January 2011.
4. U.S. Nuclear Regulatory Commission, *"Damping Values for Seismic Design of Nuclear Power Plants",* Regulatory Guide 1.61, Revision 1, March 2007.
5. Mitsubishi Heavy Industries, Ltd., *"US-APWR Concrete Outline Drawings for Inner Structure of Containment"*, NO-EHC0001 through NO-EHC0012, Revision 3, October 2010.
6. Mitsubishi Heavy Industries, Ltd., *"US-APWR Steel Plate General Arrangement Drawings"*, NO-EF30101 through NO-EF30111, Revision 0, July 2010.
7. U.S. Nuclear Regulatory Commission, *"Safety-Related Concrete Structures for Nuclear Power Plants (Other Than Reactor Vessels and Containments)",* Regulatory Guide 1.142, Revision 2, November 2001.
8. American Concrete Institute*, "Code Requirements for Nuclear Safety Related Concrete Structures"*, ACI 349-97, 1997.
9. American Concrete Institute*, "Code Requirements for Nuclear Safety Related Concrete Structures"*, ACI 349-01, February 2001.
10. American Concrete Institute*, "Code Requirements for Nuclear Safety Related Concrete Structures"*, ACI 349-06, November 2006.
11. URS Corporation, *"Basic Analysis and Design of CIS"*, Calculation CIS-13-05-230-004, Revision 0, March 2011.
12. U.S. Nuclear Regulatory Commission, *"Seismic Design Classification",* Regulatory Guide 1.29, Revision 4, March 2007.
13. URS Corporation, *"R/B Standard Design SSI Analysis"*, Calculation RB-13-05-113-002, Revision 1, June 2010.
14. Mitsubishi Heavy Industries, Ltd*., "Design Condition for Thermal Analysis of Reactor Building and PCCV"*, NO-EHB0014, Revision 3, March 2011.
15. Ozaki, M. et al., *"Study on Steel Plate Reinforced Concrete Panels Subjected to Cyclic In-Plane Shear"*, Nuclear Engineering and Design, Volume 228, 2004.
16. Sozen, M. and Moehle, J., *"Stiffness of Reinforced Concrete Walls Resisting In-Plane Shear"*, TR-102731, Electric Power Research Institute, August 1993.
17. Lee, M.J. et al., *"In-Plane Shear Behavior of Composite Steel Concrete Walls"*, 5th International Symposium on Steel Structures, March 2009.
18. Kennedy, R.P. et al., *"Engineering Characterization of Ground Motion—Task 1: Effects of Characteristics of Free-Field Motion on Structural Response"*, NUREG/CR-3805, US Nuclear Regulatory Commission, May 1984.
19. Kennedy, R.P. et al., *"Relationship Between Effective Linear Stiffness and Secant Stiffness for Pinched In-Plane Shear Behavior of Shear Walls"*, March 2011.
20. Mitsubishi Heavy Industries, Ltd., *"Damping Ratio of SC Structure"*, MUAP-10002, Revision 0, March 2010.

21. Akiyama, H. et al., *"1/10th Scale Model Test of Inner Concrete Structure Composed of Concrete Filled Steel Bearing Wall",* 10th International Conference on Structural Mechanics in Reactor Technology (SMiRT10), 1989.
22. Akita, S. et al., *"A Study on the Structural Performance of SC Thick Walls"*, Annual Conference of Architectural Institute of Japan, 2003.
23. American Society of Civil Engineers, *"Seismic Design Criteria for Structures, Systems, and Components in Nuclear Facilities"*, ASCE 43-05, May 2005.
24. U.S. Nuclear Regulatory Commission, *"Combining Modal Responses and Spatial Components in Seismic Response Analyses",* Regulatory Guide 1.92, Revision 2, July 2006.
25. American Concrete Institute*, "Reinforced Concrete Design for Thermal Effects on Nuclear Power Plant Structures"*, ACI 349.1R-07, May 2007.

LIST OF FIGURES FOR APPENDICES

LIST OF TABLES FOR APPENDICES

URS

CALCULATION SHEET

SHEET: 1 OF 13

PROJ. NO. 29427

CALC. BY: DJW DATE : 5-3-11

CHKD. BY: CTB DATE : 5-6-11

REV.: 0

PROJECT TITLE: US-APWR

SUBJECT/FEATURE: CIS Stiffness Values and Equivalent Material Properties

URS

CALCULATION SHEET

SHEET: 2 OF 13

PROJ. NO. 29427

CALC. BY: DJW DATE : 5-3-11

CHKD. BY: CTB DATE : 5-6-11

REV.: 0

PROJECT TITLE: US-APWR

SUBJECT/FEATURE: CIS Stiffness Values and Equivalent Material Properties

URS

CALCULATION SHEET

SHEET: 3 OF 13

PROJ. NO. 29427

CALC. BY: DJW DATE : 5-3-11

CHKD. BY: CTB DATE : 5-6-11

REV.: 0

PROJECT TITLE: US-APWR

SUBJECT/FEATURE: CIS Stiffness Values and Equivalent Material Properties

URS

CALCULATION SHEET

SHEET: 4 OF 13

PROJ. NO. 29427

CALC. BY: DJW DATE : 5-3-11

CHKD. BY: CTB DATE : 5-6-11

REV.: 0

PROJECT TITLE: US-APWR

SUBJECT/FEATURE: CIS Stiffness Values and Equivalent Material Properties

URS

CALCULATION SHEET

SHEET: 5 OF 13

PROJ. NO. 29427

CALC. BY: DJW DATE : 5-3-11

CHKD. BY: CTB DATE : 5-6-11

REV.: 0

PROJECT TITLE: US-APWR

SUBJECT/FEATURE: CIS Stiffness Values and Equivalent Material Properties

URS

CALCULATION SHEET

SHEET: 6 OF 13

PROJ. NO. 29427

CALC. BY: DJW DATE : 5-3-11

CHKD. BY: CTB DATE : 5-6-11

REV.: 0

PROJECT TITLE: US-APWR

SUBJECT/FEATURE: CIS Stiffness Values and Equivalent Material Properties

URS

CALCULATION SHEET

SHEET: 7 OF 13

PROJ. NO. 29427

CALC. BY: DJW DATE : 5-3-11

CHKD. BY: CTB DATE : 5-6-11

REV.: 0

PROJECT TITLE: US-APWR

SUBJECT/FEATURE: CIS Stiffness Values and Equivalent Material Properties

URS

CALCULATION SHEET

SHEET: 8 OF 13

PROJ. NO. 29427

CALC. BY: DJW DATE : 5-3-11

CHKD. BY: CTB DATE : 5-6-11

REV.: 0

PROJECT TITLE: US-APWR

SUBJECT/FEATURE: CIS Stiffness Values and Equivalent Material Properties

URS

CALCULATION SHEET

SHEET: 9 OF 13

PROJ. NO. 29427

CALC. BY: DJW DATE : 5-3-11

CHKD. BY: CTB DATE : 5-6-11

REV.: 0

PROJECT TITLE: US-APWR

SUBJECT/FEATURE: CIS Stiffness Values and Equivalent Material Properties

URS

CALCULATION SHEET

SHEET: 10 OF 13

PROJ. NO. 29427

CALC. BY: DJW DATE : 5-3-11

CHKD. BY: CTB DATE : 5-6-11

REV.: 0

PROJECT TITLE: US-APWR

SUBJECT/FEATURE: CIS Stiffness Values and Equivalent Material Properties

URS

CALCULATION SHEET

SHEET: 11 OF 13

PROJ. NO. 29427

CALC. BY: DJW DATE : 5-3-11

CHKD. BY: CTB DATE : 5-6-11

REV.: 0

PROJECT TITLE: US-APWR

SUBJECT/FEATURE: CIS Stiffness Values and Equivalent Material Properties

URS

CALCULATION SHEET

SHEET: 12 OF 13

PROJ. NO. 29427

CALC. BY: DJW DATE : 5-3-11

CHKD. BY: CTB DATE : 5-6-11

REV.: 0

PROJECT TITLE: US-APWR

SUBJECT/FEATURE: CIS Stiffness Values and Equivalent Material Properties

URS

CALCULATION SHEET

SHEET: 13 OF 13

PROJ. NO. 29427

CALC. BY: DJW DATE : 5-3-11

CHKD. BY: CTB DATE : 5-6-11

REV.: 0

PROJECT TITLE: US-APWR

SUBJECT/FEATURE: CIS Stiffness Values and Equivalent Material Properties

H. Appendix H: REFERENCES FOR APPENDICES

Booth, P.N., Varma, A.H., Malushte, S., and Johnson, W. (2007). “Experimental Behavior of Composite Sandwich Walls for Nuclear Facilities,” *Proceedings of the Annual Structural Mechanics in Reactor Technology Conference*, in press, IASMIRT, North Carolina State University, Rayleigh, NC, 10 pp.

Niwa, H., Ozaki, M., Akita, S., Takeuchi, M., Oosuga, H., and Nakayama, T. (2000). "Experimental Study on Steel-plate-reinforced Concrete Structure Part 42: Heating Tests (Thermal-Deformation Behavior). Annual Conference of Architectural Institute of Japan, 2000, Part 41-43, pp. 1127-1132.

Oosuga, H., Ozaki, M., Akita, S., Takeuchi, M., Nakayama, T., and Edo, H. (2000). "Experimental Study on Steel-plate-reinforced Concrete Structure Part 43: Heating Tests (Mechanical Aspects of SC Panels after Heating). Annual Conference of Architectural Institute of Japan, 2000, Part 41-43, pp. 1127-1132.

Ozaki, M., Akita, S., Takeuchi, M., Oosuga, H., Nakayama, T., and Niwa, H., (2000). "Experimental Study on Steel-plate-reinforced Concrete Structure Part 41: Heating Tests (Outline of Experimental Program and Results), Annual Conference of Architectural Institute of Japan, 2000, Part 41-43, pp. 1127-1132

Ozaki, M., Akita, S., Oosuga, H., Nakayama, T., Adachi, N. (2004). "Study on Steel Plate Reinforced Concrete Panels Subjected to Cyclic In-Plane Shear." Nuclear Engineering and Design, Vol. 228, pp. 225-244.

Varma, A.H., Malushte, S.R., Sener, K.C., and Booth, P.N. (2009). "Analysis and Design of Modular Composite Walls for Combined Thermal and Mechanical Loading." *Proceedings of the Annual Structural Mechanics in Reactor Technology Conference*, Division TS 6-x.y, Paper 1820, Espoo, Finland, Aug. 9-14, 2009.